Physical Properties of Graphene

Mohd Rafal Sahudin[1, 2], Muhammed Zourob[3], Muhammad Haziq Noor Akashah[2], Rozina Abdul Rani[2], Siti Rabizah Makhsin[,2]*

[1]Mechanical Engineering Branch, Public Works Department Malaysia, 50480, Kuala Lumpur, MALAYSIA
[2]School of Mechanical Engineering, College of Engineering, Universiti Teknologi MARA, 40450 Shah Alam, Selangor, MALAYSIA
[3]Department of Chemistry, Alfaisal University, Al Zahrawi Street, Al Maather, Al Takhassusi Rd, Riyadh, 11533, SAUDI ARABIA
[*]sitirabizah@uitm.edu.my

ABSTRACT

In the realm of engineering materials, a profound understanding of structural and physical characteristics holds paramount importance due to their ubiquitous presence and diverse applications. This comprehensive review delves deeply into the intricate physical attributes, commonly referred to as "physical properties," of materials based on graphene. It encompasses a wide range of aspects, including magnetic properties, optical behaviours, electrical and thermal conductivities, thickness and layer arrangements, size and shape variations, colour properties, melting points, and hardness traits. This review also explores the intriguing correlation between graphene's thickness and layering and their respective effects on its properties. Special emphasis is placed on the characterization techniques used to unveil these properties, with detailed examples from recent literature illustrating their significance. Advanced instrumentation, such as Atomic Force Microscopy (AFM), Surface Plasmon Resonance spectroscopy (SPR), Raman spectroscopy, Transmission Electron Microscopy (TEM), and X-ray Diffraction (XRD), is harnessed to provide comprehensive insights into the physical characteristics of graphene-based materials. In essence, this concise yet comprehensive review illuminates the exceptional physical properties of graphene-based materials and their potential to revolutionize various industrial sectors.

Keywords: *Physical Properties; Graphene; Mechanical Properties; Single-Layer Graphene; Multi-Layer Graphene*

ISSN 1823-5514, eISSN 2550-164X

https://doi.org/10.24191/jmeche.v12i1.24649

Received for review: 2023-09-25
Accepted for publication: 2023-10-30
Published: 2023-11-15

Introduction to Graphene

Graphene is pure carbon in one atom thick of a single layer of graphite, a very thin and nearly transparent sheet. It conducts heat and electricity with excellent efficiency, and it is extreme for its very low weight. Graphene with complex physical properties and a unique combination of bonded carbon atom structures with its myriad poised to significantly impact the future advancement of nanotechnology, electronics, material sciences, *etc* [1]. The term "physical properties of graphene" refers to the characteristics, attributes, and behaviours of graphene that can be observed and measured without altering the chemical composition of the material. These properties are primarily related to graphene's structure and how it interacts with various physical phenomena.

In general, graphene typically has great physical properties for high mobility of electrons, thermal conductivity, mechanical strength, optical transparency, and electric conductivity [2]-[3]. For instance, the demand for lightweight magnets to open new ways for flexible information storage systems design, adaptable and wearable further highlights the importance of magnetic graphene. Besides, the unbelievable potential use of graphene-based magnets in spintronics is promising, as graphene has exceptional carrier mobility and can easily integrate spin and molecular electronics [4]. Since the first graphene study was published in October 2004, over a hundred articles on graphene have appeared in prestigious journals like Science and Nature [3].

This comprehensive review article addresses a critical need in the realm of graphene research by shedding light on its multifaceted physical properties as illustrated in Figure 1. By delving deep into the intricacies of graphene-based materials, including magnetic behaviours, optical attributes, electrical and thermal conductivities, and more, it significantly contributes to our understanding of this remarkable material. The novelty of this review lies in its ability to bridge the gap between theoretical studies and experimental research, offering valuable insights that are essential for the advancement of graphene science. This comprehensive exploration of graphene's physical characteristics is particularly relevant today, as experimental researchers increasingly focus on these properties, recognizing their pivotal role in various industrial applications and cutting-edge materials research. In an era where graphene is poised to catalyse transformations in nanotechnology and materials engineering, this review article provides a clear aim and underscores its significant importance in guiding future research and applications of this extraordinary material.

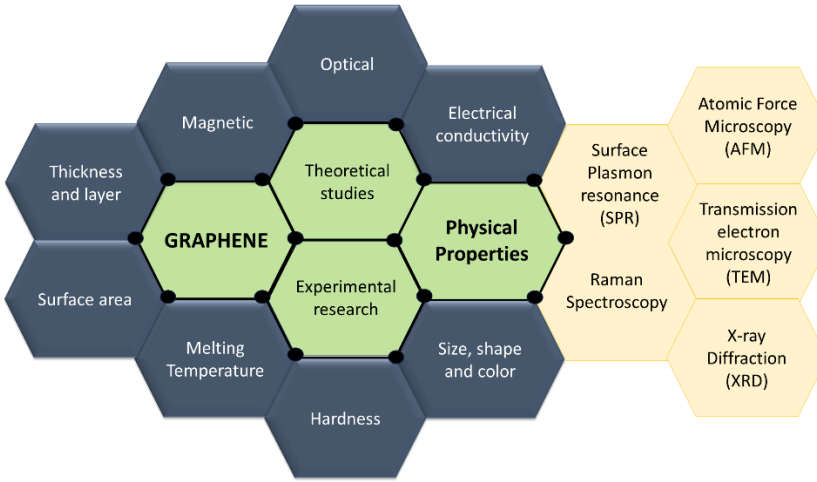

Figure 1: Overview of the content covered in the review

Thickness and Layer of Graphene

Graphene presents diverse stacking configurations, leading to various types, including monolayer or single-layer graphene (SLG), few-layer graphene (FLG), and multilayer graphene (MLG), as depicted in Figure 2. SLG comprises a lone layer of carbon atoms arranged in a hexagonal lattice, where each carbon atom forms sp^2 covalent bonds with its neighbouring atoms. This monolayer graphene is incredibly thin, consisting of just one atom's thickness.

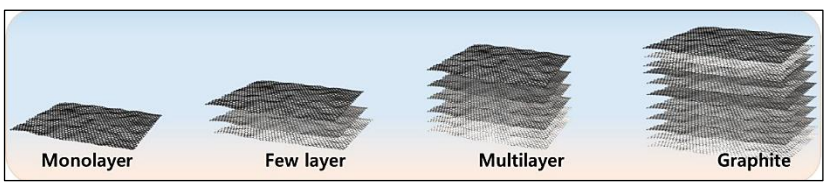

Figure 2: Schematic representation of monolayer (SLG), FLG (with ≤ 5 layers), and MLG (with ≤ 10 layers) versus graphite structure. Reproduced from [5]

The number of stacked layers plays a pivotal role in shaping the properties of graphene. For instance, SLG often exhibits superior properties when compared to both FLG and MLG [5]. SLG showcases extraordinary properties, including exceptional electrical conductivity and impressive

mechanical strength, as summarized in Table 1. SLG has an estimated 1 TPa of modulus of elasticity, a thickness range of about 1−2 nm, 2600 m^2/gr of surface area, 2.25 g/cm^3 an actual density and 4840−5300 W/mK of thermal conductivity [6]-[7].

On the contrary, FLG and MLG refer to graphene structures consisting of multiple layers of carbon atoms stacked atop each other. These layers can adopt various stacking configurations, leading to variations in MLG's properties, which depend on the number of layers and their stacking arrangement. Some types of SLG may retain some of its unique characteristics, while others may exhibit properties more akin to bulk graphite. Thicker MLG can still possess distinct attributes, although they may differ from those of SLG due to interlayer interactions. These changes encompass modifications in electronic behaviour, mechanical strength, optical transparency, and thermal conductivity, as well as the emergence of interlayer interactions and quantum effects. Each variant of graphene finds suitability for different applications [5].

Several techniques are proposed to measure the graphene thickness including one technique based on the image contrast of the graphene layers. Examples of this image contrast method include narrow-band illumination, selecting a suitable substrate, and reflection and contrast spectroscopy.

Table 1: Selected important physical and mechanical properties of single-layer graphene. Adapted with permission from [6]-[7]

Properties	Value
Bond types	sp^2
Layer number	Single layer
Crystal structure	Hexagonal
Dimension	2-D
Purity degree (%)	99
Mass (bulk) density (g/cm^3)	~0.3
Real density(g/cm^3)	2.25
Thickness (nm)	~1 – 2
Surface area (m^2/g)	2600 – 2630
High-temperature resistivity	−75 + 200 °C between not changing
Thermal conductivity (W/mK)	4840 – 5300
Electron mobility cm^2/ (V. s)	$\sim 0.015\times10^5 – 2.5\times10^5$
Elasticity module (TPa)	~0.5 – 1
Resistivity (Ω-cm)	10^{-6}
Transmittance	>95% for 2 nm thick film >70% for 10 nm thick film
Coefficient of thermal expansion	$–6\times10^{-4}$/K
Tensile strength (GPa)	130

The total colour difference (TCD) approach is a method that combines the International Commission on Illumination colour space with the reflection spectrum for accurate and rapid identification of graphene images. By restricting the light source's wavelength range, the TCD between graphene and a substrate can be improved when viewed by a regular light source [8]-[9]. Figure 3 shows an example of a TCD contour plot as a function of the number of graphene layers for different preferential dielectric films such as silicon nitride (Si_3N_4), silicon dioxide (SiO_2) and aluminium dioxide (Al_2O_3) thicknesses. Work reported by [8] improved the TCD contour of the graphene layer and substrate by narrowing the wavelength range of the light source. The outcomes of this measurement deliver a useful analysis of the graphene layer simply by measuring the different colour bands, thus showing that this technique is a non-destructive method for physical property graphene identification.

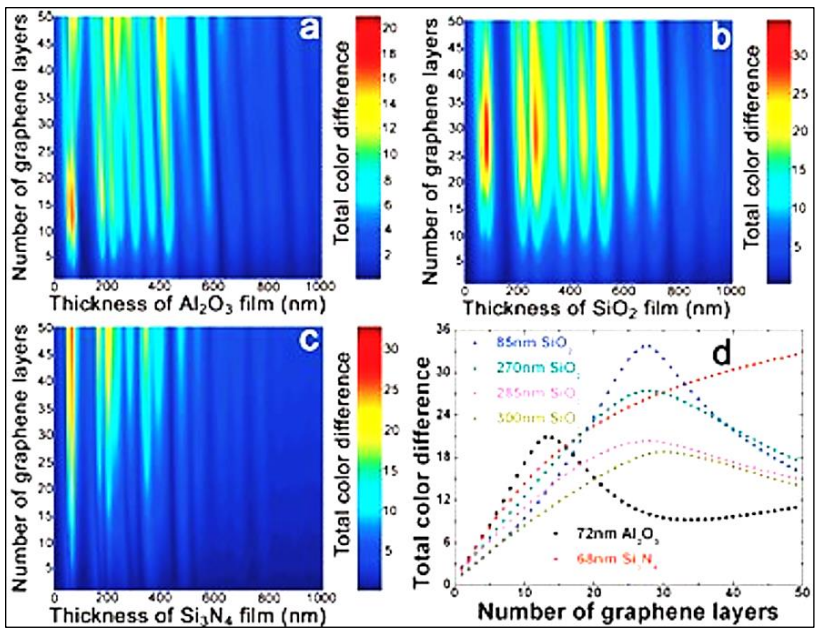

Figure 3: TCD contour plot using a different substrate with; (a) Al_2O_3 film, (b) SiO_2 film and (c) Si_3N_4 film, and (d) summary of TCD versus the number of graphene layers. Reprint with permission from [8]

[8] reported the graphene layer measurements were performed using contrast spectra for a SLG, a bi-layer and MLG on silicon (Si) substrate using SiO_2 as a capping layer and white light source. To compare the result, the calculations were made using Fresnel's reflection law and the true analysis was

obtained with a 2% standard deviation, thus showing that this contrast spectrum gives huge benefits including a straightforward, swift method for measuring graphene layers' morphology and efficiency. Later, an analytical method and a graphical method were used to calculate the number of graphene layers based on contrast spectra [9]-[11].

Furthermore, the precise determination of the number of layers and lateral dimensions of graphene film thickness can be achieved through Atomic Force Microscopy (AFM) [5], [12]. AFM is a high-resolution microscopy technique renowned for its atomic-scale resolution. It empowers the characterization of diverse material properties, including thickness, grain height, topographic features, phase diagrams, and surface roughness. Figure 4 presents topographical AFM images obtained during the measurement of SLG, two-layer graphene (2LG), and four-layer graphene (4LG). Notably, numerous adsorbed contaminants are observable on the surface of SLG (refer to Figure 4a). However, as the graphene layer count increases, these contaminants diminish, as evidenced by the topographical images from AFM (Figure 4b and 4c). This phenomenon arises from the heightened thermodynamic stability of graphene with an increasing number of layers. Specifically, the adjustment of C-C bond lengths results in the formation of wrinkles or the adsorption of molecules, which becomes notably reduced for 2LG and disappears as the graphene films become thicker [12].

[12] conducted a study utilizing AFM to determine the thickness of a graphene flake. The corresponding histogram revealed that the flake's thickness ranged from 1.1 to 1.6 nm. Considering an interlayer distance of 0.33 nm, it can be estimated that the graphene flake consists of approximately 4 to 5 layers. Consequently, it falls within the category of FLG.

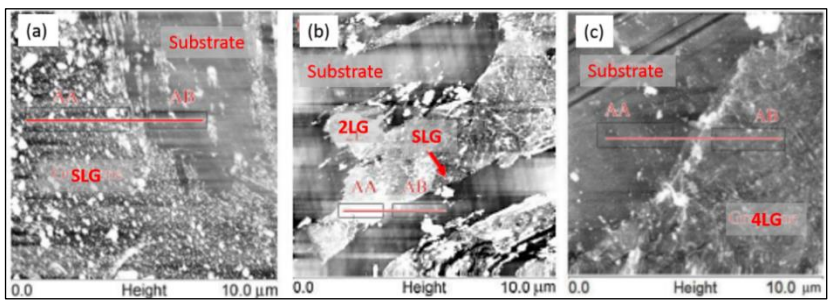

Figure 4: AFM results of topographical images for; (a) SLG, (b) 2LG, and 4LG. Reproduce with permission from [13]

The thickness of graphene film can also be measured using Surface Plasmon Resonance (SPR) as reported by [13]. SPR method is simple and well-suited for measuring thin films made from nanomaterial, although the

thickness is less than 10 nm. Their work demonstrated that the obtained SPR measurements are greatly decreased compared to AFM. The graphene film thickness was linearly increasing with an increasing number of printing cycles. Furthermore, the complex refractive index (RI) of the printed graphene flake films based on SPR provides more rigorous information on the optical absorption than that previously available using a combination of AFM and the extinction coefficient of mechanically exfoliated graphene flakes [14].

Raman spectroscopy is the foremost method for precisely assessing the average layer thickness of graphene, thanks to its exceptional sensitivity to molecular geometric structures and bonding [5], [15]-[16]. Its primary application lies in determining the number of graphene layers, as exemplified in Figure 5. The Raman spectra of graphene reveal essential insights through three key bands: the G-band (around 1587 cm^{-1}), originating from in-plane vibrational modes of sp^2 hybridized carbon atoms within the graphene sheet and highly sensitive to layer count; the D-band, which signifies defects or disorder and intensifies with increased defects, displaying resonant behaviour; and the 2D-band, consistently strong in graphene and used for layer thickness determination, relying on both its position and shape.

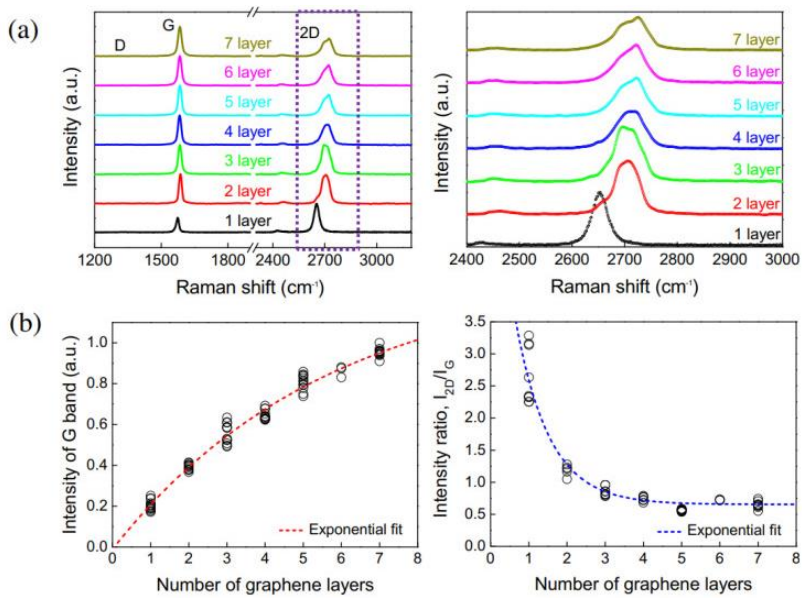

Figure 5: Example of Raman spectra of 1 to 7 layered graphenes; (a) spectral evolution of G and 2D bands, and (b) intensities of G-bands and intensity ratios of 2D vs. G bands. Reproduced with permission from [16]

Additionally, the peak intensity ratio of the 2D and G-bands aids in the identification of SLG, where a ratio of I_{2D}/I_G equalling two indicates defect-free SLG. Raman spectroscopy not only distinguishes SLG from graphite but also precisely determines layer thickness, even at atomic layer resolution. This exceptional capability establishes Raman techniques as indispensable tools in contemporary graphene research [14].

Magnetic Properties of Graphene

Magnetic materials are very useful in today's technology. It is used in data storage, power generation, and many other areas. Typical magnetic materials are metal-based including iron, cobalt, nickel, *etc*. These metals can show heavy magnetism because of their *d* and *f* electrons and can coordinate their spins to generate magnetic moments, which align along the direction of the applied magnetic fields. Almost all magnetic materials today contain elements of *3d*- or *4f*- transition metals, and they are usually ferromagnets at room temperature [4], [17]-[18].

Graphene, initially non-magnetic, has been transformed into a magnetic material through innovative techniques. Magnetic properties in graphene are closely tied to the formation of magnetic domains. Typically, ferromagnetic materials possess a single magnetic domain, where all magnetic dipoles align due to exchange energy. This energy encourages simultaneous alignment of electron spins and magnetic dipole moments. Magnetic domain formation minimizes exchange energy, enhancing material stability. Creating these magnetic domains in graphene during magnetization holds immense technological potential.

Various methods, including functionalization, doping, and atom addition, can introduce magnetism by breaking the electronic structure's symmetry locally, resulting in magnetic moments. Vacancy and edge defects offer another route to magnetization. By removing one carbon atom and rearranging others in a vacancy defect, a magnetic moment arises due to a remaining dangling bond. Experimentally, vacancy defects are created through processes like ionic bombardment and graphene oxide reduction. Among these methods, the highest magnetization occurs with sulphur and nitrogen doping, albeit at extremely low temperatures [17].

In graphene, the coexistence of π- and σ-bonding permits the carrier spin to change as well, as this change produces the magnetic property because of the lawful magnetic order. The existence of *s* and *p* electrons alone makes anticipating magnetism counterintuitive. Graphene also becomes an interesting candidate for novel spintronic devices as it has a long spin diffusion length, thus triggering a quest to incorporate the electrical and magnetic spin degrees of freedom [4]. Spintronics is considered an emerging technology based on the spin of the electron and molecular electronics associated with

magnetic moment principles, in which carbon-based magnetism could theoretically be of value [19].

However, the long-range ordering in graphene can cause complications for magnetism in 2D systems due to the lack of *d* and *f* electrons, as commonly found in conventional magnetic materials. The magnetism phenomenon can be described based on localized electronic states dependent on spin polarisation. These properties are highly affected by the state of the edge [20]. Furthermore, the graphene sheet provides a versatile medium for surface adjustments for tuning the electronic and magnetic characteristics. From *G* to *F-G-H* to *G-H* to *F-G-F* and to *H-G-H* (*G* is a graphene atom, *H* is a hydrogen atom and *F* is a fluorine atom), the properties can be tuned from nonmagnetic to magnetic, from direct gap to indirect gap or metallic to semiconducting, depending on the coverage of atoms used for the surface modification and species [21].

[22] reported on the investigation of magnetic properties, electronic properties and surface structure of the graphene layer on the lattice-matched surface of a ferromagnetic material (nickel; 111). The induced magnetic moment of the carbon atoms is evident from both spin-resolved photoemission and x-ray magnetic circular dichroism analyses. Investigations of graphene's magnetic properties are prepared by two different methods: thermal exfoliation of graphitic oxide (EG) and reducing single-layer graphene oxide (SLGO) with hydrazine hydrate. The result discloses that dominant ferromagnetic interactions coexist along with antiferromagnetic interactions in all the samples, which can be observed in phase-separated systems. The experiment concluded the magnetic properties of graphene samples depend on the area of the sample and the number of layers. As such, small values of all these variables contribute to the magnetization of the sample being greater. The magnetic properties of graphene are influenced by the molecular charge transfer that interacts with an electron donor and, thus has a greater influence than with electron-withdrawing groups like tetracyanoethylene [23].

In a study by [18], it was found that magnetism could be induced in graphene by evaporating graphene droplets under high temperatures and an external magnetic field. This innovative approach applied temperature, magnetic field, and strain simultaneously to graphene flakes, resulting in magnetization. As a consequence, all these methods led to the creation of ferromagnetic graphene powders (FGPs). The magnetization of FGPs was confirmed through measurements using a vibrating-sample magnetometer (VSM), as shown in Figure 6. This magnetic transformation can be attributed to changes in the electronic system and lattice structure of graphene. A summary of the magnetic properties of graphene is tabulated in Table 2.

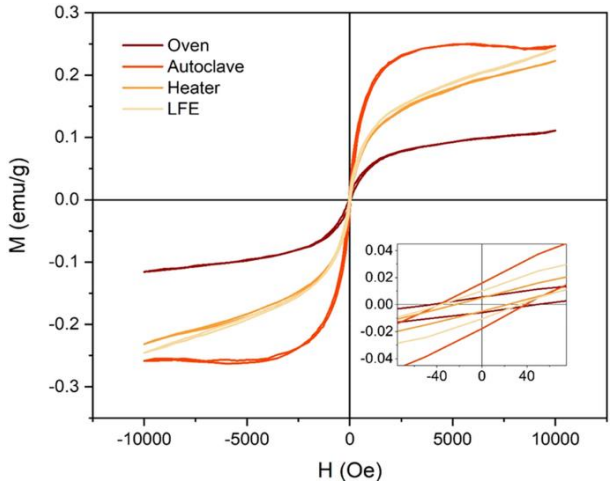

Figure 6: VSM Diagram of FGPs, illustrating the influence of temperature, pressure, and magnetic field on magnetism. The diagram includes hysteresis loops for all samples, with a zoomed-in section showing the range $-90 < H < 90$ (Oe) and $-0.045 < M < 0.045$ (emu/g) in the inset. Reproduced with permission from [18]

Table 2: Summary of graphene magnetic properties

Magnetic Property behaviour	Summary	Ref.
Methods for inducing magnetism	Functionalization, doping, and atom addition can introduce magnetism by breaking electronic symmetry.	[24]
	Vacancy and edge defects result in magnetism due to dangling bonds.	[25]
	Sulphur and nitrogen doping are effective at low temperatures.	[26]
Synthesis of Ferromagnetic Graphene Powders (FGPs)	High-temperature processes with magnetic field and strain can lead to magnetization Require high-temperature evaporation and external magnetic fields. VSM can be used to measure the magnetization of FGPs.	[27]

Optical Properties of Graphene

Graphene is composed of a monolayer of carbon atoms arranged in a honeycomb grid, where hybridized sp^2 carbon atoms form robust σ-bonds within the plane, and unhybridized p-orbitals overlap with adjacent atoms to create π-bonds. While σ-bonds primarily contribute to graphene's structural integrity, it is the π-bonds that define its optical and electronic properties. The interaction of graphene with electromagnetic radiation is especially fascinating due to the confinement of electrons in two dimensions. Graphene boasts a relatively simple band structure characterized by zero band gaps, but its optical properties are far from straightforward [22]. Unfortunately, the absence of bandgaps in graphene poses a significant challenge to its application in modern electronic components.

A simulation work reported by [28] showed that the stacking of SLG with one molybdenite monolayer formed hetero-structures generated a small bandgap around 2.5 meV showing that value can modulate for low temperature and electronic applications. In addition, this heterojunction showed some significant changes in complex dielectric function and its associated properties in the visible-light spectrum, which could be useful for future technologies and applications.

The massless Dirac fermion nature favours graphene with a universal optical response, as presented by the fine-structure constant (α) as shown in Equation 1.

$$\alpha = e^2/hc \approx 1/137.036 \quad (1)$$

where e is the electron charge, h is Planck's constant, and c is the speed of light. Experimental measurements will possibly be used to determine a fundamental constant of the universe. The graphene absorption coefficient: $\pi\alpha$ is ≈ 2.3% in the infrared region, making graphene visible without the need to observe under a microscope. The amount of light absorption may reach 10 % or even more at higher frequencies, due to van Hove singularities at the edge of the region. For graphene multilayers, the energy of visible light; $h\omega$ is around 1 to 2 eV, which is considerably higher than the Fermi energy in graphene and the electron hopping energy between graphene layers; thus, the N-layer of graphene's light absorption is Nπα [29].

Dirac Fermions in graphene are among the strongest light-matter interactions known to any system, with an optical transmission that is regulated by a constant fine structure. The pristine graphene system is a valuable testbed for table-top physics studies. On the other hand, graphene's optical properties are often commonly tuneable, either using electrical gate modulation or by the presence of defects, the effects of quantum confinement and the presence of interfacial water layers [30].

The optical properties of the electron-hole distribution of the optical excitation for the SLG have been revealed by the charge different density (CDD) method. The van der Waals interaction by edge atoms is found as a primary binding in the ground state between graphene and boron nitride as shown in Figure 7. In addition, the result of CDD shows that through optical excitation in the visual spectral region, there is no charge transfer between boron nitride and graphene. Theoretical studies reveal that for graphene-based nano-photonic applications, boron nitride is an excellent substrate for it. The findings can provide a thoughtful understanding of future optical and electrical applications of graphene/boron nitride [31]. A summary of graphene's optical properties is shown in Table 3.

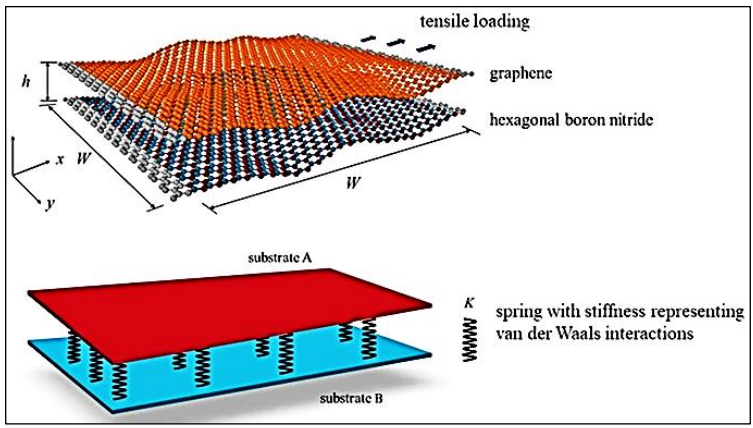

Figure 7: Van der Waals heterostructure of graphene and hexagonal boron nitride. Reprint with permission from [32]

Electrical Conductivity of Graphene

MLG has higher electrical, thermal conductivity and current-carrying potential than copper (Cu). High electrical conductivity can be generated by controlling the thickness of the MLG on an insulator formed by diffusion-controlling interlayer (IL) as first reported by [41]. This process caused the enlargement of MLG grain as the nucleation of the MLG was restrained, thus significantly affecting the crystallinity of the forming semiconductor layer. The reported electrical conductivity (2700 S/cm) was the highest measured value among other works on MLG layers and even exceeded the value of a highly oriented pyrolytic graphite (HOPG) synthesized at 3000 °C or higher.

Table 3: Summary of optical properties of graphene

Optical properties behaviour	Summary	Ref.
Generating small bandgap	Simulation work by stacking of SLG with one molybdenite monolayer formed hetero-structures generated ~2.5 meV revealing that value can modulate for low temperature and electronic applications.	[28]
Optical response	Graphene exhibits a universal optical response due to its massless Dirac fermion nature, described by the fine-structure constant (α).	[33]
Fine-structure constant (α)	$\alpha = e^2/hc \approx 1/137.036$, where e is the electron charge, h is Planck's constant, and c is the speed of light.	
Infrared absorption	The graphene absorption coefficient, $\pi\alpha$, is $\approx 2.3\%$ in the infrared region, making graphene visible without the need for microscopic observation.	[34]
Enhanced absorption at higher frequencies	Graphene can absorb over 10% of light at higher frequencies due to van Hove singularities at the edge of the region.	[35]
Graphene multilayers	For N-layer graphene, light absorption is $N\pi\alpha$, with energy levels in the visible light range (~ 1 to 2 eV).	[36]
Tuneability	Tuneable through electrical gate modulation, defects, quantum confinement, and interfacial water layers.	[37]
Charge distribution and interaction	The charge distribution reveals the primary van der Waals interaction at the ground state between graphene and boron nitride.	[38]
Charge transfer	Optical excitation in the visible spectral region shows no charge transfer between boron nitride and graphene, making boron nitride an excellent substrate for graphene-based nano-photonic applications.	[39]
Future applications	These findings provide insights into potential optical and electrical applications of graphene, particularly in combination with boron nitride.	[40]

[42] reported graphene with metal nanowires (Graphene/NW) substantially decreases the resistance of the graphene films. Graphene/NW films with a sheet resistance compared to that of the graphene's intrinsic resistance have been formed and verified as a transparent electrode substituting

one of the Indium Tin Oxides (ITO) films in ElectroChromic (EC) devices as shown in Figure 8. The result shows that the optical modulation and repeatable cycling were stable and homogenous, resulting from an integration of Graphene/NW films as a transparent electrode in EC devices, thus demonstrating their excellent potential for global optoelectronic device applications.

Conductive composites are considered for any composite that has substantial electrical conductivity, whereby the electrical conductivity can be increased by the addition of conductive fillers such as carbon-based materials including graphene into the matrix phase. The conductive filler particles begin to come into contact with each other as their content increases forming a continuous path that makes the free electrons travel easily and thus allows the composites to conduct electricity [43]-[44].

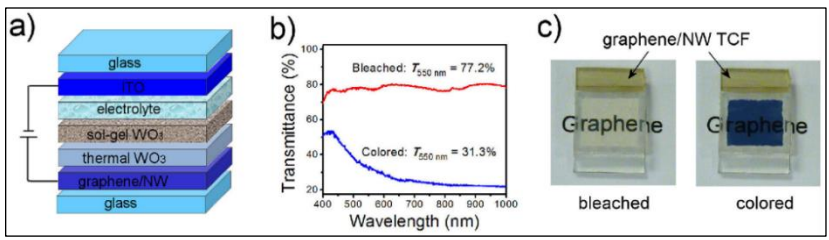

Figure 8: (a) EC device structure with one of the transparent electrodes using graphene/NW, (b) measurement of optical transmittance spectra of the EC device, and (c) the photograph of the transparent electrode of the EC device with a yellow area is a conductive silver paste consisting of Graphene/NW. Reprinted with permission from [42]

For instance, silicon nitride based (Si_3N_4) ceramics have quite notable thermal properties and mechanical properties. However, silicon nitride (Si_3N_4) also possesses electric insulators, hence the addition of 25% volume of graphene nanoplatelets (GNPs) changes the properties of these composites with the highest electrical conductivity (40 S/cm) recorded for these ceramics with added conductive particles. A desired orientation of GNPs occurs by applying plasma spark sintering by compaction and pressure-assisted densification process. As a result, the electrical conductivity measured along the direction perpendicular to the plasma spark sintering pressing axis is more than one order of magnitude higher than that measured along the parallel direction [45].

Moreover, embedding graphene into polymer matrices to form advanced multifunctional composites will dramatically enhance the electrical conductivity, elastic modulus, tensile strength and thermal conductivity to take full benefit of its application properties. Therefore, aerospace firms sought to

make conductive composites rather than metals as conductive composites are lightweight, have high strength, and have a high electrical conductivity that can protect aircraft systems from lightning strikes and electromagnetic interference [46]. A summary of graphene's electrical conductivity can be found in Table 4.

Table 4: Summary of electrical conductivity of graphene

Electrical conductivity behavior	Summary	Ref.
High electrical conductivity	MLG exhibits significantly high electrical conductivity, even surpassing highly oriented pyrolytic graphite (HOPG) synthesized at very high temperatures.	[41]
Thickness-dependence	Careful thickness control of MLG on an insulator can lead to high electrical conductivity.	[47]
Graphene with metal nanowires (Graphene/NW)	Combining graphene with metal nanowires in films results in materials with significantly reduced resistance, making them suitable as transparent electrodes in optoelectronic devices.	[48]
Conductive composites	Adding graphene to composite materials increases their electrical conductivity.	[49]
Conductive ceramics with GNPs	Incorporating GNPs into ceramics significantly enhances electrical conductivity. *E.g.* Addition of 25% volume of GNPs into Si_3N_4 changes the properties of these composites with the highest electrical conductivity of 40 S/cm.	[50]
Composite applications	Embedding graphene into polymer matrices for aerospace applications dramatically improves electrical conductivity, making them ideal for lightning strike protection and electromagnetic interference shielding.	[46, 51]

Thermal Conductivity of Graphene

The thermal conductivity, K, of a material, is defined as its capability to conduct heat. Equation 2 shows the relationship of local heat flux, q with the K with respect to the local temperature gradient, ∇T described by Fourier's law for heat conduction.

$$q = -K\nabla T \tag{2}$$

Over a wide temperature range, K is a function of T and in anisotropic materials, it relies on crystal orientation and this multi-dimensional array of numerical values can be measured by a tensor [52].

The thermal conductivity of SLG is measured in the range of 3000 – 5000 W/mK, making the value higher than the thermal conductivity of graphite (2000 W/mK). This is due to SLG being considered the basic structural component of graphite, the thermal conductivity of bulk materials comprising graphene nanoflakes is considerably supposed to be anisotropic, depending on the number of layers stacked in the sheet, the size of graphene flakes and the agglomeration state of the flakes. Thus, the thermal conductivity of graphene can be said to strongly depend on the stacking number [53].

The anisotropic bonding, and strong and low mass of the carbon atoms, make graphene and related materials unique. For example, sp^2 bonds between the carbon atoms are considered the strongest. In contrast, the adjacent graphene sheets are bonded to each other by weak van der Waals forces. This result is in agreement with [54], which also reports graphene to be highly conductive, containing a K value around 4000 W/mK.

The first simulation work performed by [56], predicted the graphene's thermal conductivity simulated at 6000 W/mK (at room temperature). Later, another experiment [55] was carried out to find the graphene's true thermal conductivity and graphene thermal conductivity to be 2000 – 4000 W/mK. Furthermore, an optical method was used to measure graphene's thermal conductivity and the reported value of thermal conductivity is about 5000 W/mK [56]-[57].

The method for measuring the thermal conductivity of graphene using confocal micro-Raman spectroscopy. Here, laser light based on the centre of the suspended graphene sheet generates heat in the graphene. Laser excitation spreads laterally through the graphene-produced heat due to the air's negligible thermal conductivity. Hence, although a small amount of heat propagated from the centre of the graphene will result in a noticeable temperature variant. Two components may describe the heat distributed from the graphene sheets' top layer: the radial heatwave and the plane-wave heat front [58].

The thermal characteristics of graphene have previously been investigated through Raman spectroscopy [38]-[40]. In these investigations, the focus was on calculating the Raman temperature shift coefficient for the G peak in graphene spectra, with an emphasis on single-layer, bi-layer, and multi-layer mechanically exfoliated graphene. The detected shift in the peak was attributed to the elongation of C-C bonds, leading to elevated stress levels, which were particularly pronounced in the case of graphene on SiO_2/Si substrates, as illustrated in Figure 9. For instance, the reactive ion etching (RIE) method was used to produce trenches on silica-based (Si/SiO_2) substrates and later, graphene was suspended over the trenches with a width of 2 – 5 μm and a depth of 300 nm [59]. Additionally, it was established that annealing graphene leads to shifts in the G, D, and 2D peaks, along with an

increase in compressive stress. Another factor contributing to the G peak shift involves lattice thermal expansion and phonon-phonon interactions [60].

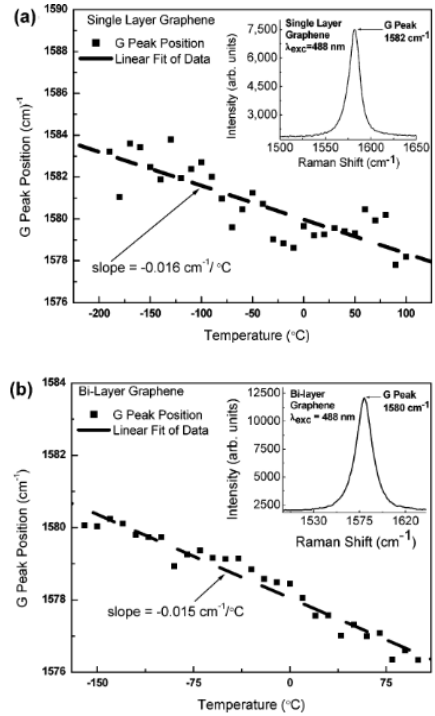

Figure 9: Temperature-dependent G-peak frequency in; (a) SLG, and (b) BLG with G-peak shape insets, and determination of the G-peak temperature coefficient. Reprint with permission from [60]

In a recent study by [61], Raman spectroscopy was employed to unveil intriguing insights about single-layered graphene's resilience at high temperatures, particularly at 600 °C. Surprisingly, it was found that the decomposition temperature of SLG exhibits a linear dependency on the coefficient of thermal expansion (CTE) of the underlying substrate. Furthermore, the study revealed distinct mechanisms governing the decomposition of graphene in different environments: air and vacuum. In both air and vacuum environments, the initiation of decomposition was linked to the extension of C-C bonds. However, a crucial distinction emerged: in the presence of oxygen in the air, the heightened strain amplified graphene's reactivity with oxygen, leading to its degradation. Conversely, in a vacuum environment, the strain alone was sufficient to induce decomposition.

The thermal conductivity (K) from the plane-wave heat front can be demonstrated in Equation 3 while for the case of the radial heatwave, Equation 4 can be used to calculate the thermal conductivity.

$$K = (L/2S)(\Delta P/\Delta T) \quad (3)$$

$$K = \chi_G(1/2h\pi)(\delta\omega/\delta P)^{-1} \quad (4)$$

Whereby L is the distance from the center of the graphene to the heat sink, $\Delta P/\Delta T$ is the changes of the heating power with respect to the temperature change and cross-sectional area, $S = h$ x W; where h is SLG thickness and W is layer width. For the temperature coefficient, χ_G is $-1.6 \times 10^{-}$ and $\delta\omega/\delta P$ designates for the slope of the G peak position shift as reflecting the heating power change.

As shown in Figure 10, the G peak excitation of Raman spectroscopy is power dependence measured for the suspended graphene layers. The increment in laser power induced an increment in the intensity of the spectra and redshift the position of the G peak. The slope from the graph in Figure 10 is represented by $\delta\omega/\delta P_D$ which is measured to be around -1.29 $cm^{-1}mW^{-1}$, where P_D is the total dissipated power [61]-[62]. When these data values are substituted into Equation 4, the thermal conductivity of freely suspended graphene is calculated at approximately 2000 ~ 4000 W/mK, which is the highest K value reported of any known material [54].

Graphene has an extraordinary thermal conductivity of up to $(5.30 \pm 0.48) \times 10^3$ W/mK measured at room temperature using a non-contact optical-based technique [59]. Measurements can be made for a SLG suspended over a large trench in the Si/SiO_2 substrate [63]-[64]. The measurements were conducted using a non-contact technique of micro-Raman spectroscopy. The quantity of power dissipated in the graphene and the subsequent temperature rise was measured from the position of the spectra and the G peak of graphene integrated intensity. The extremely high thermal conductivity in the range of 3080 – 5150 W/mK and the mean phonon-free path of around 775 nm near room temperature were determined for a set of graphene flakes [64]. This data shows that graphene as an excellent thermal management material can be applied to future nanoelectronics circuits [59].

For graphene multilayers, the weak coupling between graphene layers decreases the in-plane thermal conductivity and scatters the propagating phonons. The measurement of thermal conductivity for thicker multilayers (1 to 10 graphene layers) can approach the value of graphite in the range of 600 – 2000 W/mk. As the number of graphene layers increases from 2 to 4, the in-plane thermal conductivity drops from 2800 to 1300 W/mK [29].

The high thermal conductivity of graphene can be applied as thermal interface materials created within the composites for electronics devices which are efficient and faster in transferring the heat away from the circuits compared

to the traditional materials. For instance, [65] reported Cu/graphene nanosheet composites fabricated at 800 °C by the hot-pressing method using graphene and Cu as initial materials. Graphene content was varied from 1 %wt to 5 %wt. From the investigation of the physical properties of these composites, the relative density was found to increase by increasing the graphene content which reached the highest value at 96.78% for 5 %wt of graphene content. In addition, the composites show anisotropic properties as the pressure in the vertical direction is higher than the pressure in the parallel direction. Moreover, as the graphene content increases, the activities of thermal conductivity and electronic conductivity of the composites were decreased with the minimum of thermal conductivity and electric conductivity was measured at ~3 %wt - 4 %wt of graphene contents.

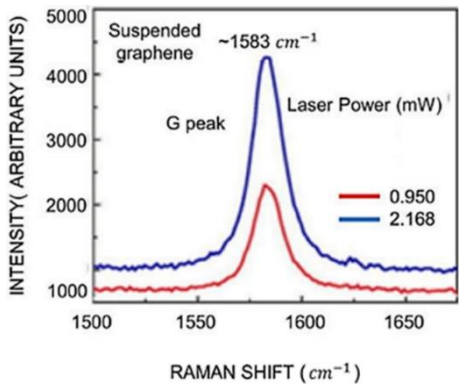

Figure 10: G-peak region counts at two different levels of power measured using Raman spectroscopy [59]

In a recent study by [71], they looked into how adding graphene nanoplatelets (GNP) to recycled polycarbonate (PC) affects thermal properties. The results showed that GNP had little impact on thermal stability and glass transition temperature (T_g) for both virgin and recycled PC when compared to PC without GNP. Recycled PC was weaker and less heat-resistant than virgin PC, but it improved when mixed with GNP. The best thermal stability for virgin PC/GNP composites came with 1 %wt GNP (a 2.74% increase), while recycled PC/GNP composites achieved their highest thermal stability at 10 %wt GNP (a 2.42% increase). However, recycled PC-based composites were less thermally stable than virgin PC-based composites under the same GNP loading. T_g for virgin PC/GNP initially increased with 1 wt.-% GNP and then decreased with more GNP. For recycled PC/GNP, T_g showed irregular changes with GNP loading. A comprehensive summary of graphene's thermal conductivity is presented in Table 5.

Table 5: Summary of thermal conductivity of graphene

Thermal conductivity behaviour	Summary	Ref.
Single layer of graphene (SLG)	SLG exhibits high thermal conductivity in the range of 3000 - 5000 W/mK, surpassing that of graphite (2000 W/mK).	[65]
Anisotropic thermal conductivity	The thermal conductivity of graphene depends on crystal orientation, making it anisotropic. This anisotropy is contingent on several factors, including the number of layers stacked in the sheet, the size of graphene flakes, and the agglomeration state of the flakes.	[59], [64]-[66]
Multilayer of graphene (MLG)	It is evident that the thermal conductivity of graphene is influenced by the stacking number of layers. The weak coupling between graphene layers decreases the in-plane thermal conductivity and scatters the propagating phonons. E.g. the measurement of K for thicker multilayers (1 to 10 graphene layers) can approach the value of graphite in the range of 600 – 2000 W/mk.	[29]
Strong carbon bonds	Graphene's strong sp^2 carbon bonds contribute to its high thermal conductivity.	[59]
Variability in reported values	Experimental measurements of graphene's thermal conductivity have reported values ranging from 2000 to 6000 W/mK.	[67]
Measurement techniques	Often measured using techniques such as confocal micro-Raman spectroscopy.	[68]
Composite applications	The high thermal conductivity of graphene makes it suitable for thermal management materials in electronic devices.	[69]
Graphene Nanoplatelets (GNP) in Polycarbonate Composites (PC)	The addition of GNP to recycled PC enhances thermal stability and glass transition temperature, offering the potential for composite applications.	[70]

Size, Shape, and Colour of Graphene

There are many ways to characterize graphene and find its properties, such as using spectroscopy techniques including Raman spectroscopy, X-ray

diffraction [71], TEM [72], *etc*. [73] reported that by examining using TEM, graphene was observed as a transparent figure and stable under high energy electrons in contrast to GO was observed as semi-transparent which is not stable under high energy beam. Here, the morphology of GO was demonstrated as a thick, rough surface with flat flake layers, irregular in-shape with non-uniform particle size and not crumpled. However, a graphene sheet film was observed with a thin flat flake with crumpled morphology and composed of a wrinkled flake structure.

In Figure 11, a low-magnification TEM image provides a glimpse of graphene nanosheets. These nanosheets, some spanning hundreds of square nanometers, appear perched atop the copper grid, resembling the delicate, undulating waves of crumpled silk veils. The graphene nanosheets exhibit a rippled and interwoven structure, creating a mesh-like appearance. Remarkably, they maintain their transparency and structural stability when exposed to the electron beam. In Figure 11a, the most transparent and unremarkable regions, indicated by arrows, are likely monolayer graphene nanosheets. Additionally, Figure 11b reveals the presence of scrolled graphene nanosheets in the sample [48].

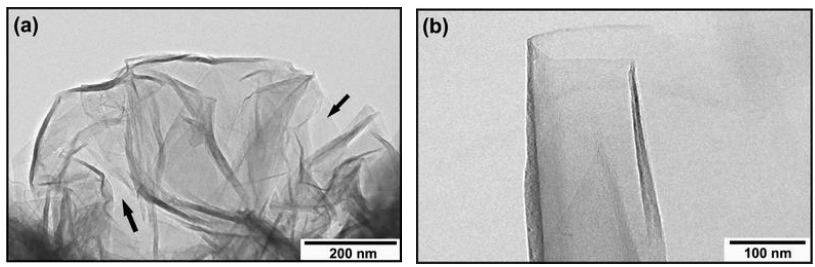

Figure 11: (a) TEM characterization of graphene nanosheets – low magnification overview resembling crumpled silk with arrows showing mono-layer (SLG), and (b) a close-up of scrolled nanosheet structures. Reproduced with permission from [48]

Dynamic dispersion of light is a simple and fast method of characterizing the size of the graphene nanosheets and the exfoliated graphene oxide [73]. This method is more reliable for spherical particles [74] and the dynamic dispersion of light would not measure the particle size of graphene nanomaterial if the sample is polydisperse [75].

Furthermore, two methods have started emerging in recent years to characterize nanoparticles: nanoparticle tracking analysis and asymmetric flow field-flow fractionation. Nanoparticle tracking analysis has given an average size of ca. 150 nm and higher resolution than dynamic dispersion of light and approximate concentrations. It has been indicated that the dynamic dispersion of light given the average particle size of graphene which the intensity was a

bias towards larger particles. Asymmetric flow field-flow fractionation separated different populations of graphene nanosheets with different gyration radii (centered at approximately 360 nm) and provided information on the graphene structure and shape of the particles [76]-[77].

Other characterization such as XRD can be used to determine the number of graphene layers. For instance, the average number of graphene layers decreased from 15 to 3 as the average sp^2 crystallite size decreased from 17.33 nm to 14.75 nm. Moreover, the increased ID/IG ratio from Raman spectroscopy measurement demonstrated an increase in the quantity of sp^2 domains with the defect density increment after reduction [78].

The graphene color deposited on the substrates can be found using an imaging microscope and AFM measurements [79]-[81]. The TCD method (as described in detail in the previous section: Thickness and Layer of Graphene) of assessment assesses the color difference between the graphene layer and the underlying substrate. With this technique, one can figure out the most viable thickness of the dielectric layer (the single layer of metals and insulators or the layered structure) to ensure the optimum optical transparency of a graphene-based multilayer.

Colour is a useful technique for visual analysis. It can be beneficial when detecting and judging the thickness of graphene and multilayer approaches [81]. The data on the colors of graphene and GO were confirmed by the method of an optical microscope and profilometer. Here, GO has a lower extinction coefficient than graphene, which causes the reflectance of GO to fluctuate more clearly over a range of material thicknesses. Consequently, the resulting colors of GO changed continually as a function of the material thickness. However, the colors of the graphene multilayer became saturated without periodic change.

In summary, manipulating and visualizing the optical contrast of SLG and other 2D materials will lead to new knowledge about the various aspects of light and matter interactions with atomic thickness. The optical properties of SLG can be tuned by gating, and it can be demonstrated and manipulated in color contrast. Another important potential application is in ultra-thin, versatile color displays. Under white light using broadband photon management, scalable large-area color displays the novel chromatic color contrast optical visibility of SLG. The optical absorption of SLG on fused quartz (SiO_2) substrate is drastically enlarged to more than 10 % from ∼1.4 at wavelength, λ of the scan range between 560 − 990 nm (from yellow to near-infrared spectral regimes). The current process is much more appealing without the excessive artificial color utilized with SLG [82]. The characterization methods employed to determine the size, shape, and color of graphene are summarized in Table 6.

Table 6: Summary of characterization method in determining size, shape and colour of graphene

Characterization method	Summary	Ref.
Size measurement (dynamic dispersion of light)	Methods like nanoparticle tracking analysis and flow field fractionation provide size and shape details	[83]
Number of layers (XRD and Raman)	Determines layer count based on crystallite size of XRD spectrum. Thicker graphene layers exhibit a higher ID/IG ratio in Raman spectroscopy, indicating a greater number of defects or discontinuities in their structure compared to single-layer graphene (SLG) measurements.	[84]-[85]
Color-thickness correlation (Microscopy and AFM)	TCD method assesses the color difference between the graphene layer and the substrate.	[9]

Hardness of Graphene

The hardness-displacement and elastic module-displacement curves in various graphene layers can be measured using nano-indentation as shown in Figure 12. A large dip is found to be below 10 nm in the depth range and the curves are increasing progressively to stability. An additional continuous rigidity calculation (CSM) demonstrates an inflected depth of 10 nm. The load-displacement curve also shows that the load decreases with an increment of layers at the same indentation depth. Figure 12 also illustrates that both graph hardness and the graphene elastic modulus decrease as the number of graphene layers increases. The layers of graphene were further confirmed through AFM images, as depicted in Figure 12d, which show a range from a single layer at spot A to more than four layers at spot E, respectively.

Because of its superior mechanical properties, graphene can be considered an ideal reinforcement to produce composites so that the hardness can be improved. These features provide an increased opportunity to study metal matrix composites. [87] reported that they made mechanical alloys to study the composites. The time used for milling was 1 hour, 3 hours, and 5 hours. In an aluminium (Al) powder matrix, graphene nanoplatelets (GNPs) were added at concentrations of 0.25, 0.50, and 1.0 %wt. The Al coating on graphene delayed the formation of amorphous graphene structures as the milling time increased. Milling time and the presence of GNPs have a beneficial effect on hardness values. The mechanical behaviour of the

hardness-assessed GNP/Al composites shows that increased milling time leads to harder compounds being produced at a sintering time of 2 hours.

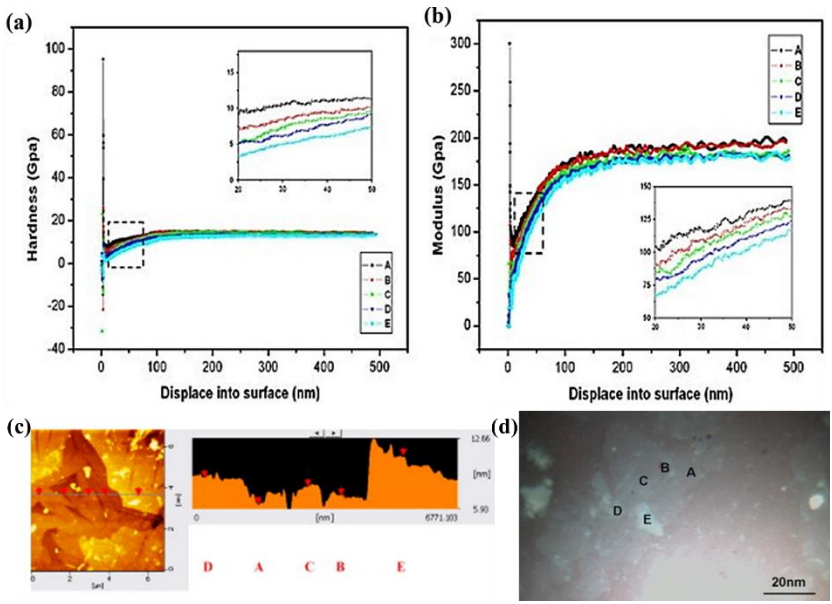

Figure 12: (a) Hardness–displacement, (b) elastic modulus–displacement graph, and (c) AFM of graphene measured on various spots as in (d) optical microscope image of graphene on the Si substrate [86]

Graphene reinforced with Al-based metal matrix composites has also been developed successfully using stir casting technology which retains the graphene loading rate of 0.5, 1, 1.5, and 2 %wt. The hardness number of the rocks well is found by testing all prepared specimens. The conclusion was that the sample filled with 0.5 %wt graphene shows the maximum indentation resistance because the graphene is uniformly dispersed into the aluminium matrix. Graphene particles enhance the hardness of the soft matrix and record 78 Rockwell hardness numbers (RHN) in relation to the parental composition. The minimum hardness figure is also found in the sample that has 2 %wt graphene because graphene particles are overloaded as the parental atoms have difficulty replacing them when cooled down, and the graphene particle saturation limit that fills the aluminium matrix is emphasized. Consequently, the material cannot bear more load to find its response to indentation[87].

[89] also reported on developing different graphene-enhanced (GNP) reinforced titanium (Ti) composites using the powder metallurgy (PM) process. As a result, GNPs GNP-reinforced Ti composites have improved hardness, microstructure, and density properties for optimal process

parameters. The highest hardness (566 HV) and density (4.39 g/cm^3) were achieved for the right amount of GNP at 1100 ºC for 120 min (0.15 %wt). Meanwhile, Ti composites reduced their density and hardness when GNPs content was above 0.15 %wt because of the GNPs agglomeration trend. Better atomic motion and diffusion at optimal time and temperature are positive for Ti composite characteristics. However, density, hardness, and structure deteriorated due to the damage to GNP structure and titanium carbide (TiC) formation at high-content GNPs. Over 0.30 %wt of the undesired TiC was detected. In comparison to pure Ti, the hardness of the Ti–GNPs composite increased from 304 HV to 566 HV because of fine-grain strengthening mechanisms and dislocation. A summary of graphene`s hardness is tabulated in Table 7.

The Melting Temperature of Graphene

For a first phase transition from 2D solid to 3D liquid, the melting of graphene is based on the nucleation theory. Because these two phases have different dimensions, it is difficult to determine the free energy difference between them, and thus it is unclear how to describe the melting temperature (T_m). T_m is a well-defined temperature as the point at which the liquid and solid phases of Gibb's free energy curves intersect. Here, a 2D nucleation theory shows how this difficulty can be overcome and gives T_m a reliable quantitative value. Spontaneous melting of graphene occurs at a temperature known as T^*_m of 4900 K, providing an upper limit of T_m for graphene. Nucleation theory can explain the melting of bulk graphene, allowing for an unambiguous definition of the T_m, which is 4510 K, approximately 250 K higher than that of graphite and currently the highest of all materials [93].

Furthermore, atomic simulations are used to study high-temperature graphene behaviour based on an exact atomic carbon potential. As a result, the aggregation of Stone–Wales defects and the formation of octagons are the initial stages of the melting process, which is carried out via the formation of carbon chains. Rather than being a simple liquid, the molten state is a 3D network of entangled chains. The melting temperature is approximately 4900 K, as determined by the extrapolation of simulation and 2D Lindemann criterion and results for various heating rates [94].

Table 7: Summary of the hardness properties of graphene with respect to various compositions added to the graphene

Graphene-composite	Hardness properties	Ref.
Graphene layers	Hardness and elastic modulus were measured using nano-indentation. A large dip is observed at depths below 10 nm. The load-displacement curve shows a decrease in load with increased layers at the same indentation depth. Graph hardness and elastic modulus decrease with increasing graphene layers.	[89]
Copper coated graphene reinforced aluminium composites (Cu-GNP-Al)	With the introduction of 0.5 %vol graphene, the composite material displays a tensile strength of 242 MPa and demonstrates a conductivity of 34.5 MS/m. This signifies a noteworthy improvement, with an increase of 102% in tensile strength and approximately 8.15% in conductivity compared to the characteristics of pure aluminium manufactured under the same conditions.	[90]
Graphen Aluminium Composites (GNP-Al)	Graphene was added to the aluminium powder matrix to form composites. Milling time and the presence of GNPs positively affect hardness values. Increased milling time results in harder compounds, especially with 2 hours of sintering. Stir casting technology was used to create composites with different graphene loadings. Uniform graphene dispersion enhances hardness. A sample with 0.5 %wt graphene shows maximum indentation resistance, achieving a hardness of 78 RHN. Samples with 2 %wt graphene exhibit reduced hardness due to graphene particle overload and agglomeration.	[90] [91]
Graphene-Ti Composites (Ti-GNP)	GNP-reinforced Ti composites developed using the powder metallurgy process. The right amount of GNP at 0.15 %wt achieves the highest hardness (566 HV) and density (4.39 g/cm^3) at 1100 ºC for 120 min. Higher GNP content results in reduced density and hardness due to agglomeration and TiC formation. The hardness of Ti-GNPs composite increases from 304 HV to 566 HV compared to pure Ti.	[92]

[96] reported the dynamic properties and structure of bulk materials consisting of graphene nanosheets using simulations of coarse-grain molecular dynamics. Results demonstrate convincing evidence of fluid-like melts of linear polymers at elevated temperatures in bulk graphene. In addition, at temperatures below the glass transfer temperature (T_g), the materials transform into a glassy "foam" condition. Due to the high T_g (≈ 1600 K) of bulk graphene materials in their glassy foam state, they have high thermal stability and an enormous free volume compared to standard polymer materials. This shows that the lubricating properties and attractive plastic flow at high temperatures are in graphene melting. Additionally, graphene foams show great promise as high-surface-area fire suppression additives and filtration materials for mechanical reinforcement and increasing the thermal conductivities of polymer materials.

Atomic simulations were used to investigate the melting behaviour of graphene-supported pure platinum (Pt), pure palladium (Pd), Pt-core/Pd-shell (Pt@Pd), and Pdcore/Pt-shell (Pd@Pt) nanoparticles (NPs) of the same size. The melting point of supported NPs is approximately 120 K lower than the free melting point. This can be attributed to restrictions of NPs by raising the temperature and distortions at the interface between metal and carbon on the graphene support. The analysis shows that the graphene support does not significantly impact melting modes because of the low distortion in the structure of the nanoparticles [97].

In addition, computer simulation has been used to study the dynamics of graphene disordering upon heating. Seeds in the 3D liquid stage form with heating graphene due to a complex disruption sequence and the formation of many interatomic bonds. Because of the 5-7 defects, groups of adjacent rings, and big rings and carbon chains perpendicular to the monolayer floor appear in the final stage. Although Stone–Wale (SW) defects occur, they do not accumulate, soon become rinsed, and have no significant impact on the melting mechanism. During the melting process, disordered and crystalline regions coexist. From the above, the melting point is estimated at 5100 K. To conclude, high graphene thermal stability is essential in real-world applications, for instance, visible light emitters based on thermal radiation resulting from solid sample heating [98]. The melting temperature behaviours of graphene are summarized in Table 8.

The Surface Area of Graphene

Graphene is supposed to have outstanding properties, such as a high specific surface area, and excellent electrical and thermal conductivity [101]. Graphene nanoplates are ideal nanomaterial compared to other nanoparticles of metal oxide or conventional metal because they have a very high specific surface area. It is recognized as the world's thinnest material and has significant

application potential in various technologies, including liquid crystal devices. [102] reported graphene has an extremely high specific surface area, and it is a highly effective additive for promoting the heterogeneous nucleation of water. A minimal amount of graphene can eliminate the degree of water subcooling. With a surface area concentration of about 0.070 ± 0.003 m^2/ml and a meagre mass fraction of about 0.020 ± 0.001 wt% of graphene, the need for subcooling to freeze water was eliminated as shown in Figure 13. Surfactants can be used to decrease the degree of subcooling, increase suspension stability, and slightly increase the total freezing time.

Table 8: Summary of graphene's melting temperatures in relation to defects and mixing with other materials

Material	Melting Temperature (K)	Ref.
Graphene (2D Nucleation Theory)	4510 K, about 250 K higher than that of graphite based on nucleation theory for a first order phase transition from the 2D solid to the 3D liquid via an intermediate quasi-2D liquid.	[94]
High-temperature graphene (atomistic simulations)	Stone-Wales (SW) defects are pivotal in governing graphene's melting temperature, with the aggregation of these defects triggering the formation of octagons. These octagons act as precursors for the spontaneous melting process, which occurs at approximately Tm ≈ 4900 K.	[95]
Graphene nanosheets (simulations of coarse-grain molecular dynamics)	Approx. 1600 K (T_g), graphene foams show great promise as high-surface-area fire suppression additives and filtration materials	[96]
Graphene-supported nanoparticles (simulation)	Approx. 120 K lower than the free melting point	[97], [99]
Graphene disorder upon heating (simulation)	5100 K	[98], [100]

Graphene composites, more specifically polymer matrix composites, are among the most profitable industrial products in various applications. The current state of the study of surface characteristics of graphene is predominant in graphene composite applications. The influence factors of surface characteristics of graphene, such as surface energy, microstructure, surface chemistry and composition, surface area, surface chemistry, and the techniques used for determining the graphene surface characteristics [103].

The properties of composites are mainly determined by the synergistic combination of concrete graphene surface, high interface adhesion of filler matrix, and exceptional characteristics of graphene and the main features of the matrix [104]. The conclusions showed that graphene surface characteristics could be adapted to better compatibility by altering graphene surface chemistry and improving interfacial interaction by increasing the surface area and wrinkling by mechanically interlocking. Furthermore, the chemical bonds on the graphene surface by functional groups like van der Waals and hydrogen bonding, result in a decrease in graphene dispersive surface energy while improving graphene wettability for the matrix. Modified graphene with unique surface properties would result in better composites considering the desired lifespan of high-performance reinforced materials [103].

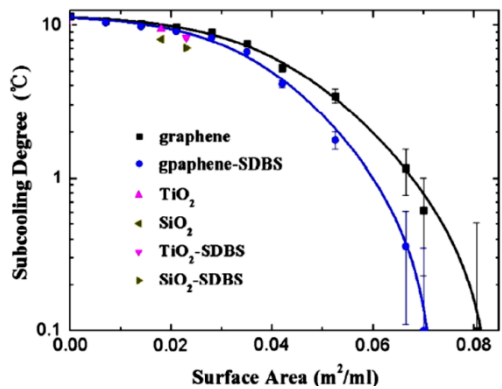

Figure 13: Relationship between graphene–H_2O nanofluids subcooling degree and the surface area per volume of samples [102]

The porous graphene materials have been given significant attention in recent years and rapidly developing because of their excellent electrochemical performances, larger surface areas, and unique pore structures in conversion and storage devices. Due to these extraordinary properties, porous graphene materials can be used as critical components in high-performance conversion devices and electrochemical energy storage such as fuel cells, lithium-ion batteries, and supercapacitors. Although the application and synthesis of porous materials have significantly progressed, a few significant points are left to be addressed. There is also an exciting challenge in developing porous graphene materials because it is necessary to precisely control pore morphology, including wall thickness. In addition, the interaction of various pores, such as mesopores, macropores, and micropores, is necessary for utilizing the synergistic effects of multiple pores [105].

The surface porosity of graphene-based aerogels plays a critical role in their performance in applications involving mass transfer. Many applications

of graphene-based aerogels, including but not limited to energy storage, gas sensing, chemical adsorption, and catalysis, crucially rely on efficient mass transfer processes. However, understanding the factors that determine surface porosities has been a challenge, impeding their optimization for specific applications. [106] have introduced an innovative approach to control surface porosity, which is essential for enhancing the performance of 3D-printed aerogels. They highlight the significance of ink properties, typically adjusted through additives in graphene oxide (GO) suspensions, and print parameters in shaping the surface porosity of graphene-based aerogels. Through a combination of experiments and hydrodynamic simulations, they demonstrate that the high shear stress experienced during the 3D printing process leads to a non-porous surface, whereas crosslinking of the sheets inhibits flake alignment induced by shearing, resulting in a porous surface (see Figure 14). These findings provide valuable insights for precise control of the surface porosity in printed graphene-oxide aerogels (GOA) by regulating crosslinking agents and shear stress.

Conclusions

In conclusion, graphene stands as a formidable force poised to exert a transformative influence across multiple scientific disciplines and technological domains. Its unparalleled amalgamation of bonded carbon structures, underpinned by a plethora of intricate physical attributes, positions it as a cornerstone of innovation. These remarkable properties span its thickness, layering, magnetic and optical characteristics, electrical and thermal conductivity, supercapacitance, hardness, and more. The inherent potential in these properties extends to diverse applications, ranging from cutting-edge sensor devices to integrated circuit components and beyond. Particularly captivating is the optical absorption behaviour of single-layer graphene (SLG), which is exclusively governed by a fundamental constant of nature, rendering it truly distinctive. This peculiarity signifies a noteworthy departure from frequency-dependent materials, solidifying its significance in the scientific landscape.

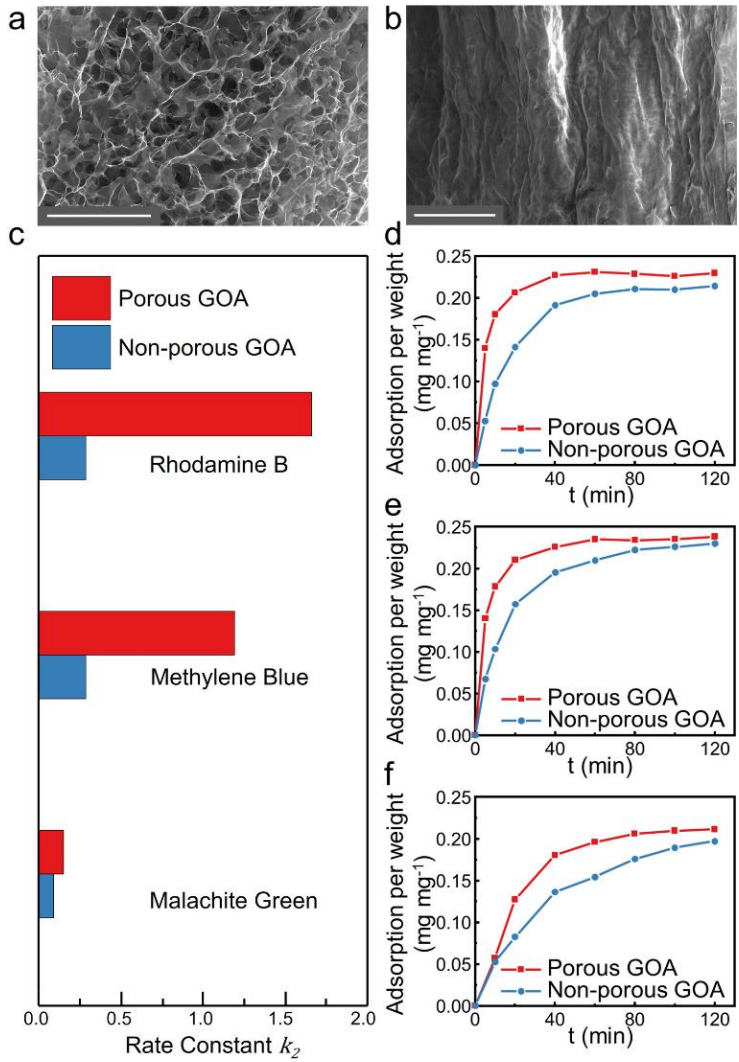

Figure 14: Comparative examination of surface structures and dye adsorption performance in porous and non-porous graphene oxide aerogels (GOA). SEM images of the surface of; (a) porous GOA, (b) non-porous GOA with scale bars of 100 μm, (c) rate constants derived from adsorption kinetics fitting. (d)–(f) Dye adsorption curves of porous GOA and non-porous GOA for; (d) rhodamine B, (e) methylene blue, and (f) malachite green. Reprinted with permission from [106]

Moreover, the development of graphene films unveils a suite of exceptional physical properties that underpin its promise in advanced applications. These include its potential as a high-power system component and an efficient heat-spreading material, offering novel avenues for thermal management within form factor-driven electronics. In essence, the exceptional attributes of graphene and its far-reaching implications underscore its pivotal role in shaping the future of various scientific disciplines and driving technological advancements. Its unique blend of structural and physical characteristics not only fuels curiosity in research but also holds the promise of revolutionizing industries and enhancing our understanding of the fundamental properties of matter.

Future Outlooks

To unlock the full potential of graphene in today's research and development landscape, fostering collaboration among researchers from diverse scientific fields is essential. These collaborations serve as a catalyst for innovative solutions, addressing complex challenges and contributing to our evolving understanding of graphene's physical properties. They underscore graphene's pivotal role in shaping the present and future of science and technology across a range of domains.

Given the growing importance of graphene in both scientific and industrial contexts, a pressing need exists for comprehensive assessments of the environmental impact of graphene-based materials and technologies. These assessments are crucial not only for sustainability but also for managing potential risks associated with the expanding production and application of graphene. To enhance awareness and appreciation of graphene's significance, it's highly advisable to establish educational initiatives and outreach programs targeting both the scientific community and the general public. These efforts have the potential to broaden understanding and recognition of graphene's extraordinary properties and its transformative impact across various industries.

Moreover, when designing applications, understanding graphene's physical properties is a crucial initial step. However, the effects of heterogeneity and defects on chemical interactions and graphene's properties require further investigation. For instance, the complexity of transport in multilayer graphene, influenced by multiple conducting layers, and the challenges of achieving precise atom-by-atom functionalization of graphene on large-area graphene wafers warrant in-depth research. Further exploration of graphene's integration into existing materials and engineering processes is vital, aligning with current trends in material science and engineering.

Efforts to explore comprehensive, reliable, and large-scale graphene production should be undertaken. A key challenge is scaling up the production

of high-quality graphene, which significantly impacts material properties. The production parameters should align with the chosen method or route. Moreover, characterizing graphene products at an industrial scale is crucial. Techniques such as XRD, Raman spectroscopy, X-ray photoelectron spectroscopy (XPS), and additional specialized characterizations for parameters like surface area and electrical conductivity should be considered.

Lastly, the establishment of standardized protocols and stringent quality control measures for graphene production and characterization is essential in today's rigorous research and industrial environments. These measures are critical for ensuring consistency and reliability in graphene-related studies, fostering confidence and uniformity in the field. Graphene's exceptional properties continue to offer ongoing opportunities for researchers to explore its potential, driving advancements across various fields in alignment with the current state of research and development in graphene and materials science.

Contributions of Authors

The authors confirm the equal contribution in each part of this work. All authors reviewed and approved the final version of this work. Mohd Rafal: Data curation, Writing – original draft. Mohamed Zourob; Review Muhammad Haziq Noor Akashah: Writing – original draft and correction, Rozina Abdul Rani: Writing – review & Siti Rabizah Makhsin: Validation, Supervision, Writing – review & editing, formatting, submission.

Funding

This work is financially supported by the GIP grant UiTM (600-RMCGIP5/3(106/2022)).

Conflict of Interests

All authors declare that they have no conflicts of interest.

Acknowledgment

The authors would like to acknowledge all the support from the School of Mechanical Engineering, UiTM Shah Alam, Malaysia.

References

[1] T. M. Radadiya, E. Journal, M. S. Vol, E. Centre, and D. Uk, "A properties of graphene," European Journal of Material Sciences, vol. 2, no. 1, pp. 6–18, 2015. [Online]. Available: https://www.eajournals.org/wp-content/uploads/A-Properties-of-Graphene.pdf (Accessed May 14, 2022).

[2] I. Jung, J.-S. Rhyee, J. Y. Son, R. S. Ruoff, and K.-Y. Rhee, "Colors of graphene and graphene-oxide multilayers on various substrates," *Nanotechnology*, vol. 23, no. 2, p. 025708, 2011. https://doi.org/10.1088/0957-4484/23/2/025708.

[3] M. H. Noor Akashah, M. R. Sahudin, R. A. Rani, P. J. Scully, and S. R. Makhsin, "Chemical properties of graphene," in Woodhead Publishing Series in Electric and Optical Materials, 2022, pp. 43-67. https://doi.org/10.1016/B978-0-323-85457-3.00023-2

[4] N. Tang, T. Tang, H. Pan, Y. Sun, J. Chen, and Y. Du, "Chapter 6 - Magnetic properties of graphene," in Spintronic 2D Materials, W. Liu and Y. Xu, Eds., Elsevier, 2020, pp. 137–161. https://doi.org/10.1016/B978-0-08-102154-5.00005-9

[5] N. Parvin, V. Kumar, S. W. Joo, S.-S. Park, and T. K. Mandal, "Recent advances in the characterized identification of mono-to-multi-layer graphene and its biomedical applications: A Review," *Electronics*, vol. 11, no. 20, p. 3345, 2022. https://doi.org/10.3390/electronics11203345

[6] O. Guler and N. Bagci, "A short review on mechanical properties of graphene reinforced metal matrix composites," *Journal of Materials Research and Technology*, vol. 9, no. 3, pp. 6808–6833, 2020. https://doi.org/10.1016/j.jmrt.2020.01.077

[7] H. G. P. Kumar and M. A. Xavior, "Graphene reinforced metal matrix composite (GRMMC): A Review," *Procedia Engineering*, vol. 97, pp. 1033–1040, 2014. https://doi.org/10.1016/j.proeng.2014.12.381

[8] L. Gao, W. Ren, F. Li, and H. M. Cheng, "Total color difference for rapid and accurate identification of graphene," *ACS Nano*, vol. 2, no. 8, pp. 1625–1633, 2008. https://doi.org/10.1021/nn800307s

[9] S. Reshmi, R. Sundheep, and D. J. Late, "Optical Based Techniques for 2D Layered Materials," in Advanced Analytical Techniques for Characterization of 2D Materials, AIP Publishing, 2022. https://doi.org/10.1063/9780735425422_002

[10] Z. H. Ni, H. M. Wang, J. Kasim, H. M. Fan, T. Yu, Y. H. Wu, Y. P. Feng, and Z. X. Shen, "Graphene thickness determination using reflection and contrast spectroscopy," *Nano Letters*, vol. 7, no. 9, pp. 2758–2763, 2007. https://doi.org/10.1021/nl071254m

[11] M. Tahriri, M. D. Monico, A. Moghanian, N. T. Yaraki, R. Torres, A. Yadegari, and L. Tayebi, "Graphene and its derivatives: Opportunities

and challenges in dentistry," *Materials Science and Engineering: C*, vol. 102, pp. 171–185, 2019. https://doi.org/10.1016/j.msec.2019.04.051

[12] X. Xu, S. Sun, J. Luo, R. Ma, J. Lin, L. Fang, P. Zhang, and Y. Chen, "Few-layer graphene prepared via microwave irradiation of black sesame for supercapacitor applications," *Chemical Engineering Journal*, vol. 425, p. 130664, 2021. https://doi.org/10.1016/j.cej.2021.130664

[13] Y. Yao, L. Ren, S. Gao, and S. Li, "Histogram method for reliable thickness measurements of graphene films using atomic force microscopy (AFM)," *Journal of Materials Science & Technology*, vol. 33, no. 8, pp. 815–820, 2017. https://doi.org/10.1016/j.jmst.2016.07.020

[14] H. Jussila, T. A. Owen, H. Yang, G. Hu, S. Aksimsek, N. Granqvist, H. Lipsanen, R. C. T. Howe, Z. Sun, and T. Hasan, "New approach for thickness determination of solution-deposited graphene thin films," *ACS Omega*, vol. 2, no. 6, pp. 2630–2638, 2017. https://doi.org/10.1021/acsomega.7b00336

[15] M. Wall, "The raman spectroscopy of graphene and the determination of layer thickness," Semantic Scholar, 2011. Available: https://api.semanticscholar.org/CorpusID:13670837 (Accessed Oct. 31, 2023).

[16] Y. Hwangbo, C. K. Lee, A. E. M. Isa, J. W. Jang, H. J. Lee, S. B. Lee, S. S. Kim, and J. H. Kim, "Interlayer non-coupled optical properties for determining the number of layers in arbitrarily stacked multilayer graphenes," *Carbon*, vol. 77, pp. 454–461, 2014. https://doi.org/10.1016/j.carbon.2014.05.050

[17] S. Trivedi, K. Lobo, and H. S. S. R. Matte, "Synthesis, Properties, and Applications of Graphene," in Woodhead Publishing Series in Electronic and Optical Materials, Fundamentals and Sensing Applications of 2D Materials, Woodhead Publishing, pp. 25–90, 2019. https://doi.org/10.1016/B978-0-08-102577-2.00003-8

[18] M. Alimohammadian and B. Sohrabi, "Observation of magnetic domains in graphene magnetized by controlling temperature, strain and magnetic field," *Scientific Reports*, vol. 10, no. 1, p. 21325, 2020. https://doi.org/10.1038/s41598-020-78262-w

[19] O. Hod, V. Barone, and G. E. Scuseria, "Half-metallic graphene nanodots: A comprehensive first-principles theoretical study," *Physical Review B*, vol. 77, no. 3, p. 035411, 2008. https://doi.org/10.1103/physrevb.77.035411

[20] T. Enoki and K. Takai, "The edge state of nanographene and the magnetism of the edge-state spins," *Solid State Communications*, vol. 149, no. 27–28, p. 1144–1150, 2009. https://doi.org/10.1016/j.ssc.2009.02.054

[21] J. Zhou, M. M. Wu, X. Zhou, and Q. Sun, "Tuning electronic and magnetic properties of graphene by surface modification," *Applied*

Physicals Letters, vol. 95, no. 10, 2009. https://doi.org/10.1063/1.3225154

[22] Y. S. Dedkov and M. Fonin, "Electronic and magnetic properties of the graphene-ferromagnet interface," *New Journal of Physics*, vol. 12, no. 12, 2010. https://doi.org/10.1088/1367-2630/12/12/125004

[23] H. S. S. Ramakrishna Matte, K. S. Subrahmanyam, and C. N. R. Rao, "Novel magnetic properties of graphene: Presence of both ferromagnetic and antiferromagnetic features and other aspects," *Journal of Physical Chemistry C*, vol. 113, no. 23, p. 9982–9985, 2009. https://doi.org/10.1021/jp903397u

[24] Z. Li, S. Li, Y. Xu, and N. Tang, "Recent advances in magnetism of graphene from 0D to 2D," *Chemical Communications*, vol. 59, no. 42, pp. 6286–6300, 2023. https://doi.org/10.1039/D3CC01311A

[25] O. V. Yazyev and L. Helm, "Defect-induced magnetism in graphene," *Physical Review B*, vol. 75, no. 12, p. 125408, 2007. https://doi.org/10.1103/physrevb.75.125408

[26] G. Vignesh, P. Devendran, N. Nallamuthu, S. Sudhahar, P. S. Kumar, and M. K. Kumar, "Effects of nitrogen, sulphur, and temperature treatments on the spectral, structural, and electrochemical characteristics of graphene oxide for energy storage applications," *Carbon Trends*, vol. 11, p. 100262, 2023. https://doi.org/10.1016/j.cartre.2023.100262

[27] A. Saren, V. Laitinen, M. Vinogradova, and K. Ullakko, "Twin boundary mobility in additive manufactured magnetic shape memory alloy 10M Ni-Mn-Ga," *Acta Materialia*, vol. 246, p. 118666, 2023. https://doi.org/10.1016/j.actamat.2022.118666

[28] G. Ulian, D. Moro, and G. Valdrè, "Electronic and optical properties of graphene/molybdenite bilayer composite," *Composite Structures*, vol. 255, p. 112978, 2021. https://doi.org/10.1016/j.compstruct.2020.112978

[29] Z. Xu, Fundamental properties of graphene. Elsevier Inc., 2017. https://doi.org/10.1016/B978-0-12-812651-6.00004-5

[30] M. Kavitha and M. Jaiswal, "Graphene: A review of optical properties and photonic applications", *Asian Journal of Physics*, vol. 25, no. 7, p. 809–831, 2016, Available: https://home.iitm.ac.in/manu.jaiswal/AJP%20Optical%20Prop%20Graphene.pdf (Acessed Oct 31, 2023).

[31] J. Wang, S. Cao, P. Sun, Y. Ding, Y. Li, and F. Ma, "Optical advantages of graphene on the boron nitride in visible and SW-NIR regions," *RSC Advances*, vol. 6, no. 112, p. 111345–111349, 2016. https://doi.org/10.1039/c6ra24588a

[32] H. Qin, Y. Liang, and J. Huang, "Size and temperature effect on the mechanical properties of graphene/hexagonal boron nitride van der Waals heterostructure*," Materials Science Engineering: B*, vol. 265, p. 115006, 2021. https://doi.org/10.1016/j.mseb.2020.115006

[33] R. Shimano, G. Yumoto, J. Y. Yoo, R. Matsunaga, S. Tanabe, H. Hibino, T. Morimoto, and H. Aoki, "Quantum faraday and kerr rotations in graphene," *Nature Communications*, vol. 4, no. 1, p. 1841, 2013. https://doi.org/10.1038/ncomms2866

[34] Q. Li, J. Lu, P. Gupta, and M. Qiu, "Engineering Optical Absorption in Graphene and Other 2D Materials: Advances and Applications," *Advanced Optical Materials*, vol. 7, no. 20, p. 1900595, 2019. https://doi.org/10.1002/adom.201900595

[35] R. Debbarma, S. K. Behura, Y. Wen, S. Che, and V. Berry, "WS2-induced enhanced optical absorption and efficiency in graphene/silicon heterojunction photovoltaic cells," *Nanoscale*, vol. 10, no. 43, pp. 20218–20225, 2018. https://doi.org/10.1039/c8nr03194k

[36] W. Li, G. Cheng, Y. Liang, B. Tian, X. Liang, L. Peng, A. R. H. Walker, D. J. Gundlach, N. V. Nguyen, "Broadband optical properties of graphene by spectroscopic ellipsometry," *Carbon*, vol. 99, pp. 348–353, 2016. https://doi.org/10.1016/j.carbon.2015.12.007

[37] M. H. Tsai, Y. X. Lu, C. Y. Lin, C. H. Lin, C. C. Wang, C. M. Chu, W. Y. Woon, and C. T. Lin, "The first-water-layer evolution at the graphene/water interface under different electro-modulated hydrophilic conditions observed by suspended/supported field-effect-device architectures," *ACS Applied Materials & Interfaces*, vol. 15, no. 13, pp. 17019–17028, 2023. https://doi.org/10.1021/acsami.3c00037

[38] W. Aggoune, C. Cocchi, D. Nabok, K. Rezouali, M. Akli Belkhir, and C. Draxl, "Enhanced light–matter interaction in graphene/h-bn van der waals heterostructures," *The Journal of Physical Chemistry Letters*, vol. 8, no. 7, pp. 1464–1471, 2017. https://doi.org/10.1021/acs.jpclett.7b00357.

[39] A. Kuzmina, M. Parzefall, P. Back, T. Taniguchi, K. Watanabe, A. Jain, and L. Novotny, "Resonant light emission from graphene/hexagonal boron nitride/graphene tunnel junctions," *Nano Letters*, vol. 21, no. 19, pp. 8332–8339, 2021. https://doi.org/10.1021/acs.nanolett.1c02913

[40] J. Wang, F. Ma, W. Liang, and M. Sun, "Electrical properties and applications of graphene, hexagonal boron nitride (h-BN), and graphene/h-BN heterostructures," *Materials Today Physics*, vol. 2, pp. 6–34, 2017, https://doi.org/10.1016/j.mtphys.2017.07.001

[41] H. Murata, Y. Nakajima, N. Saitoh, N. Yoshizawa, T. Suemasu, and K. Toko, "High-electrical-conductivity multilayer graphene formed by layer exchange with controlled thickness and interlayer," *Scientific Reports*, vol. 9, no. 1, pp. 1–5, 2019, https://doi.org/10.1038/s41598-019-40547-0

[42] I. N. Kholmanov, C. W. Magnuson, A. E. Aliev, H. Li, B. Zhang, J. W. Suk, L. L. Zhang, E. Peng, S. H. Mousavi, A. B. Khanikaev, R. Piner, G. Shvets, and R. S. Ruoff, "Improved electrical conductivity of graphene films integrated with metal nanowires," *Nano Letters*, vol. 12, no. 11, pp. 5679–5683, 2012, https://doi.org/10.1021/nl302870x

[43] B. Alemour, M. H. Yaacob, H. N. Lim, and M. R. Hassan, "Review of electrical properties of graphene conductive composites," *International Journal of Nanoelectronics and Materials*, vol. 11, no. 4, pp. 371–398, 2018.

[44] V. B. Mohan, K. Lau, D. Hui, and D. Bhattacharyya, "Graphene-based materials and their composites: A review on production, applications and product limitations," *Composites Part B: Engineering*, vol. 142, pp. 200–220, 2018.https://doi.org/10.1016/j.compositesb.2018.01.013

[45] C. Ramirez, F. M. Figueiredo, P. Miranzo, P. Poza, and M. I. Osendi, "Graphene nanoplatelet/silicon nitride composites with high electrical conductivity," *Carbon*, vol. 50, no. 10, pp. 3607–3615, 2012. https://doi.org/10.1016/j.carbon.2012.03.031

[46] B. Alemour, O. Badran, and M. R. Hassan, "A Review of Using Conductive Composite Materials in Solving Lightening Strike and Ice Accumulation Problems in Aviation," *Journal of Aerospace Technology and Management*, vol. 11, pp. 1–23, 2019. https://doi.org/10.5028/jatm.v11.1022

[47] I. Torres, S. M. Aghaei, N. Pala, and A. Gaitas, "Selective area multilayer graphene synthesis using resistive nanoheater probe*," Scientific Reports*, vol. 13, no. 1, 2023. https://doi.org/10.1038/s41598-023-34202-y

[48] G. Wang, J. Yang, J. Park, X. Gou, B. Wang, h. Liu, and J. Yao, "Facile synthesis and characterization of graphene nanosheets," *The Journal of Physical Chemistry C*, vol. 112, no. 22, pp. 8192–8195, 2008. https://doi.org/10.1021/jp710931h

[49] F. A. Chyada, A. R. Jabur, and H. A. Alwan, "Effect addition of graphene on electrical conductivity and tensile strength for Recycled electric power transmission wires," *Energy Procedia*, vol. 119, pp. 121–130, 2017. https://doi.org/10.1016/j.egypro.2017.07.055

[50] Y. Tan, H. Luo, H. Zhang, and S. Peng, "Graphene nanoplatelet reinforced boron carbide composites with high electrical and thermal conductivity," *Journal of The European Ceramic Society*, vol. 36, no. 11, pp. 2679–2687, 2016. https://doi.org/10.1016/j.jeurceramsoc.2016.04.036

[51] B. Zhang, S. A. Soltani, L. N. Le, and Ramazan Asmatulu, "Fabrication and assessment of a thin flexible surface coating made of pristine graphene for lightning strike protection," *Materials Science and Engineering: B*, vol. 216, pp. 31–40, 2017. https://doi.org/10.1016/j.mseb.2017.02.008

[52] J. H. Warner, F. Schäffel, A. Bachmatiuk, and M. H. Rümmeli, "Chapter 3 - Properties of Graphene," in Graphene, Elsevier, 2013, pp. 61–127. https://doi.org/10.1016/B978-0-12-394593-8.00003-5

[53] K. Takai, S. Tsujimura, F. Kang, and M. Inagaki, "Chapter 6 - Thermal properties and applications," in Graphene, Elsevier, 2020, pp. 415–447. https://doi.org/10.1016/B978-0-12-819576-5.00006-2

[54] M. Sang, J. Shin, K. Kim, and K. J. Yu, "Electronic and thermal properties of graphene and recent advances in graphene based electronics applications," *Nanomaterials*, vol. 9, no. 3, pp. 1–33, 2019. https://doi.org/10.3390/nano9030374

[55] Q. F. Cheng, J. P. Wang, J. J. Wen, C. H. Liu, K. L. Jiang, Q. Q. Li, S. and S. Fan, "Carbon nanotube/epoxy composites fabricated by resin transfer molding," *Carbon*, vol. 48, no. 1, pp. 260–266, 2010. https://doi.org/10.1016/j.carbon.2009.09.014

[56] J. K. W. Sandler, J. E. Kirk, I. A. Kinloch, M. S. P. Shaffer, and A. H. Windle, "Ultra-low electrical percolation threshold in carbon-nanotube-epoxy composites," *Polymer*, vol. 44, no. 19, pp. 5893–5899, 2003. https://doi.org/10.1016/S0032-3861(03)00539-1

[57] M. D. Siti Hajar, A. Ghani. Supri, and J. A. Jalil, "Effect of carbon black loading on tensile properties, electrical conductivity and swelling behavior of poly(vinyl) chloride/polyethylene oxide conductive films," *Applied Mechanics and Materials*, vol. 679, pp. 128–131, 2014. https://doi.org/10.4028/www.scientific.net/amm.679.128

[58] J. Shiomi and S. Maruyama, "Non-fourier heat conduction in a single-walled carbon nanotube: classical molecular dynamics simulations," *Physical Review B*, vol. 73, no. 20, pp. 1–7, 2006. https://doi.org/10.1103/PhysRevB.73.205420

[59] A. A. Balandin, S. Ghosh, W. Bao, I. Calizo, D. Teweldebrhan, F. Miao, and C. N. Lau, "Superior thermal conductivity of single-layer graphene," *Nano Letters*, vol. 8, no. 3, pp. 902–907, 2008. https://doi.org/10.1021/nl0731872

[60] I. Calizo, A. A. Balandin, W. Bao, F. Miao, and C. N. Lau, "Temperature dependence of the raman spectra of graphene and graphene multilayers," *Nano Letters*, vol. 7, no. 9, pp. 2645–2649, 2007, https://doi.org/10.1021/nl071033g

[61] L. Průcha, M. Lejeune, M. Kizovský, and E. Materna-Mikmeková, "In-situ thermal Raman spectroscopy of single-layer graphene on different substrates," *Materials Today Communications*, vol. 35, p. 105921, 2023. https://doi.org/10.1016/j.mtcomm.2023.105921

[62] A. A. Balandin, S. Ghosh, W. Bao, I. Calizo, D. Teweldebrhan, F. Miao, and C. N. Lau, "Extremely High Thermal Conductivity of Graphene: Experimental Study," *Nano Letters*, vol. 8, no. 3, pp. 902-907, 2008. https://doi.org/10.1109/SNW.2008.5418404

[63] H. Malekpour and A. A. Balandin, "Raman-based technique for measuring thermal conductivity of graphene and related materials," *Journal of Raman Spectroscopy*, vol. 49, no. 1, pp. 106–120, 2017. https://doi.org/10.1002/jrs.5230

[64] A. A. Balandin, S. Ghosh, W. Bao, I. Calizo, D. Teweldebrhan, F. Miao, and C. N. Lau, "Extremely high thermal conductivity of graphene: Prospects for thermal management applications in nanoelectronic

circuits," *Applied Physics Letters*, vol. 92, no. 15, pp. 1–4, 2008. https://doi.org/10.1063/1.2907977

[65] B. W. Wei, D. Qu, C. F. Hu, F. Z. Li, T. L. Zhou, R. Jun Xie, Z. M. Zhou, "Synthesis and physical properties of graphene nanosheets reinforced copper composites," *Advanced Materials Research*, vol. 833, pp. 310–314, 2014. https://doi.org/10.4028/www.scientific.net/AMR.833.310

[66] A. Li, C. Zhang, Y. F. Zhang, "Thermal conductivity of graphene-polymer composites: mechanisms, properties, and applications," Polymers, vol. 9, no. 12, p. 437, 2017. https://doi.org/10.3390/polym9090437

[67] S. Norouzi and M. M. Seyyed Fakhrabadi, "Anisotropic nature of thermal conductivity in graphene spirals revealed by molecular dynamics simulations," *Journal of Physics and Chemistry of Solids*, vol. 137, p. 109228, 2020. https://doi.org/10.1016/j.jpcs.2019.109228

[68] J. Renteria, D. Nika, and A. Balandin, "Graphene thermal properties: applications in thermal management and energy storage," *Applied Sciences*, vol. 4, no. 4, pp. 525–547, 2014. https://doi.org/10.3390/app4040525

[69] K. Bera, D. Chugh, Aditya Bandopadhyay, Hark Hoe Tan, A. Roy, and Chennupati Jagadish, "Decoupling the roles of defects/impurities and wrinkles in thermal conductivity of wafer-scale hBN films," *Journal of Applied Physics*, vol. 134, no. 15, 2023. https://doi.org/10.1063/5.0168186

[70] Y. Fu, J. Hansson, Y. Liu, S. Chen, A. Zehri, M. K. Samani, N. Wang, Y. Ni, Y. Zhang, and Z. B. Zhang, "Graphene related materials for thermal management," *2D Materials*, vol. 7, no. 1, p. 012001, 2019. https://doi.org/10.1088/2053-1583/ab48d9

[71] D. Wijerathne, Y. Gong, S. Afroj, N. Karim, and C. Abeykoon, "Mechanical and thermal properties of graphene nanoplatelets-reinforced recycled polycarbonate composites," *International Journal of Lightweight Materials and Manufacture*, vol. 6, no. 1, pp. 117–128, 2023. https://doi.org/10.1016/j.ijlmm.2022.09.001

[72] D. F. Báez, H. Pardo, I. Laborda, J. F. Marco, C. Yáñez, and S. Bollo, "Reduced graphene oxides: Influence of the reduction method on the electrocatalytic effect towards nucleic acid oxidation," *Nanomaterials*, vol. 7, no. 7, 2017. https://doi.org/10.3390/nano7070168

[73] M. Aziz, F. S. A. Halim, and J. Jaafar, "Preparation and characterization of graphene membrane electrode assembly," *Jurnal Teknologi*, vol. 69, no. 9, pp. 11–14, 2014. https://doi.org/10.11113/jt.v69.3388

[74] M. Lotya, A. Rakovich, J. F. Donegan, and J. N. Coleman, "Measuring the lateral size of liquid-exfoliated nanosheets with dynamic light scattering," *Nanotechnology*, vol. 24, no. 26, 2013. https://doi.org/10.1088/0957-4484/24/26/265703

[75] S. Badaire, P. Poulin, M. Maugey, and C. Zakri, "In situ measurements of nanotube dimensions in suspensions by depolarized dynamic light scattering," *Langmuir*, vol. 20, no. 24, pp. 10367–10370, 2004. https://doi.org/10.1021/la049096r

[76] H. Kato, A. Nakamura, and S. Kinugasa, "Effects of angular dependency of particulate light scattering intensity on determination of samples with bimodal size distributions using dynamic light scattering methods," *Nanomaterials*, vol. 8, no. 9, 2018. https://doi.org/10.3390/nano8090708

[77] J. Amaro-gahete, A. Ben, and D. Esquivel, "A comparative study of particle size distribution of graphene nanosheets synthesized by an ultrasound-assisted method," *Nanomaterials*, vol. 9, no. 2, p. 152, 2019. https://doi.org/10.3390/nano9020152

[78] Y. G. Andreev and P. G. Bruce, "Size and shape of graphene layers in commercial carbon blacks established by Debye refinement," *Journal of Applied Crystallography*, vol. 49, no. 1, pp. 24–30, 2016. https://doi.org/10.1107/s1600576715021378

[79] A. Kaushal, S. K. Dhawan, and V. Singh, "Determination of crystallite size, number of graphene layers and defect density of graphene oxide (GO) and reduced graphene oxide (RGO)," *Nucleation and Atmospheric Aerosols*, vol. 2115, pp. 1–5, 2019. https://doi.org/10.1063/1.5112945

[80] J. Kim, F. Kim, and J. Huang, "Seeing graphene-based sheets," *Materials Today*, vol. 13, no. 3, pp. 28–38, 2010. https://doi.org/10.1016/s1369-7021(10)70031-6.

[81] S. Roddaro, P. Pingue, V. Piazza, V. Pellegrini, and F. Beltram, "The optical visibility of graphene: interference colors of ultrathin graphite on SiO_2," *Nano Letters*, vol. 7, no. 9, pp. 2707–2710, 2007. https://doi.org/10.1021/nl071158l

[82] I. Jung, J. S. Rhyee, J. Y. Son, R. S. Ruoff, and K. Y. Rhee, "Colors of graphene and graphene-oxide multilayers on various substrates," *Nanotechnology*, vol. 23, no. 2, 2012. https://doi.org/10.1088/0957-4484/23/2/025708

[83] X. Yu, S. Fu, Y. Song, H. Wang, X. Wang, J. Kong, and J. Liu, "Color contrast of single-layer graphene under white light illumination induced by broadband photon management," *ACS Applied Materials & Interfaces*, vol. 12, no. 3, pp. 3827–3835, 2019. https://doi.org/10.1021/acsami.9b16149

[84] L. E. Crica, T. J. Dennison, E. A. Guerini, and K. Kostarelos, "A method for the measurement of mass and number of graphene oxide sheets in suspension based on non-spherical approximations," *2D Materials*, vol. 8, no. 3, pp. 035044–035044, 2021. https://doi.org/10.1088/2053-1583/abfe01

[85] S. H. Huh, "X-ray diffraction of multi-layer graphenes: Instant measurement and determination of the number of layers," *Carbon*, vol. 78, pp. 617–621, 2014. https://doi.org/10.1016/j.carbon.2014.07.034

[86] Y. Zhang and C. Pan, "Measurements of mechanical properties and number of layers of graphene from nano-indentation," *Diamond and Related Materials*, vol. 24, pp. 1–5, 2012. https://doi.org/10.1016/j.diamond.2012.01.033

[87] R. Pérez-Bustamante, D. Bolaños-Morales, J. Bonilla-Martínez, I. Estrada-Guel, and R. Martínez-Sánchez, "Microstructural and hardness behavior of graphene-nanoplatelets/aluminum composites synthesized by mechanical alloying," *Journal of Alloys and Compounds*, vol. 615, pp. S578–S582, 2014. https://doi.org/10.1016/j.jallcom.2014.01.225

[88] T. Pinto and Umesh, "Influence of graphene on hardness number of Aluminium-7075 based metal matrix composites," *International Journal of Innovative Science and Research Technology*, vol. 2, no. 12, pp. 285–289, 2017.

[89] M. Gürbüz and T. Mutuk, "Effect of process parameters on hardness and microstructure of graphene reinforced titanium composites," *Journal of Composite Materials*, vol. 52, no. 4, pp. 543–551, 2017. https://doi.org/10.1177/0021998317745143

[90] Y. Luo, Y. Huang, J. Liu, and Q. Chen, "Copper coated graphene reinforced aluminum composites with enhanced mechanical strength and conductivity," *Vacuum*, vol. 218, p. 112610, 2023. https://doi.org/10.1016/j.vacuum.2023.112610

[91] P. Lava Kumar, A. Lombardi, G. Byczynski, S. V. S. Narayana Murty, B. S. Murty, and L. Bichler, "Recent advances in aluminium matrix composites reinforced with graphene-based nanomaterial: A critical review," *Progress in Materials Science*, vol. 128, p. 100948, 2022. https://doi.org/10.1016/j.pm atsci.2022.100948

[92] R. Ranjan, N. Kumar Singh, A. Prakash Jaiswal, and V. Bajpai, "Metal matrix nano composites using graphene nano platelets indented on copper particles in aluminium matrix," *Advanced Materials Letters*, vol. 9, no. 09, pp. 652–655, 2018. https://doi.org/10.5185/amlett.2018.2078

[93] W. Zhang, S. Zhou, W. Ren, Y. Yang, L. Shi, Q. Zhou, and M. Liu, "Uniformly dispersing GNPs for fabricating graphene-reinforced pure Ti matrix composites with enhanced strength and ductility," *Journal of Alloys and Compounds*, vol. 888, p. 161527, 2021. https://doi.org/10.1016/j.jallcom.2021.161527

[94] J. H. Los, K. V. Zakharchenko, M. I. Katsnelson, and A. Fasolino, "Melting temperature of graphene," *Physical Review B*, vol. 91, no. 4, pp. 1–6, 2015. https://doi.org/10.1103/PhysRevB.91.045415

[95] K. V. Zakharchenko, A. Fasolino, J. H. Los, and M. I. Katsnelson, "Melting of graphene: from two to one dimension," *Journal of Physics: Condensed Matter*, vol. 23, no. 20, pp. 202202–202202, 2011. https://doi.org/10.1088/0953-8984/23/20/202202

[96] W. Xia, F. Vargas-Lara, S. Keten, and J. F. Douglas, "Structure and dynamics of a graphene Melt," *ACS Nano*, vol. 12, no. 6, pp. 5427–5435, 2018. https://doi.org/10.1021/acsnano.8b00524

[97] B. Mobedpour, S. Rajabdoust, and R. Roumina, "Melting of graphene supported Pd-Pt core-shell nanoparticles: A molecular dynamics study," *Computational Materials Science*, vol. 151, pp. 132–143, 2018. https://doi.org/10.1016/j.commatsci.2018.05.010

[98] L. A. Openov and A. I. Podlivaev, "On graphene melting," *Physics of The Solid State*, vol. 58, no. 4, pp. 847–852, 2016. https://doi.org/10.1134/S1063783416040168

[99] Q. Zheng, Z. Tian, T. Gao, Y. Liang, Q. Chen, and Q. Xie, "Effect of graphene on solid–liquid coexistence in Cu nanodroplets," *Applied Surface Science*, vol. 637, p. 157952, 2023. https://doi.org/10.1016/j.apsusc.2023.157952

[100] S. Subrina and D. Kotchetkov, "Simulation of heat conduction in suspended graphene flakes of variable shapes," *Journal of Nanoelectronics and Optoelectronics*, vol. 3, no. 3. pp. 249–269, 2008. doi: 10.1166/jno.2008.303.

[101] L. Li, X. Zhang, J. Qiu, B. L. Weeks, and S. Wang, "Reduced graphene oxide-linked stacked polymer forests for high energy-density supercapacitor," *Nano Energy*, vol. 2, no. 5, pp. 628–635, 2013, https://doi.org/10.1016/j.nanoen.2013.07.011

[102] L. Xing, Y. Chen, Z. Cheng, L. Jia, S. Mo, and Z. Liu, "Ultrahigh specific surface area of graphene for eliminating subcooling of water," *Applied Energy*, vol. 130, pp. 824–829, 2014. https://doi.org/10.1016/j.apenergy.2014.02.032

[103] J. F. Dai, G. J. Wang, L. Ma, and C. K. Wu, "Surface properties of graphene: Relationship to graphene-polymer composites," *Reviews on Advanced Materials Science*, vol. 40, no. 1, pp. 60–71, 2015.

[104] J. Longun, G. Walker, and J. O. Iroh, "Surface and mechanical properties of graphene-clay/polyimide composites and thin films," *Carbon*, vol. 63, pp. 9–22, 2013. https://doi.org/10.1016/j.carbon.2013.06.024

[105] S. Han, D. Wu, S. Li, F. Zhang, and X. Feng, "Porous graphene materials for advanced electrochemical energy storage and conversion devices," *Advanced Materials*, vol. 26, no. 6, pp. 849–864, 2014. https://doi.org/10.1002/adma.201303115

[106] B. Zhou, Z. Chen, Q. Cheng, M. Xiao, G. Bae, D. Liang, and T. Hasan, "Controlling surface porosity of graphene-based printed aerogels," *2D Materials and Applications*, vol. 6, no. 1, pp. 1–8, 2022. https://doi.org/10.1038/s41699-022-00312-w